# ABSTRACT

Title of the Dissertation: MICROSTRUCTURAL CHANGES UNDER ISOTHERMAL AGING AND THEIR INFLUENCE ON THERMAL FATIGUE RELIABILITY FOR TIN-LEAD AND LEAD-FREE SOLDER JOINTS, INCLUDING MICROSTRUCTURAL CHANGES UNDER ISOTHERMAL AGING IN MIXED SOLDER JOINTS

Anupam Choubey, Doctor of Philosophy, 2007

Directed by: Professor Michael G. Pecht

Department of Mechanical Engineering

Most electronics companies have transitioned to lead-free processes, both to comply with government legislation and to avoid issues related to mixing of tin-lead and lead-free metallurgies. However, exemptions from lead-free legislation have been granted for certain products, especially those intended for high-reliability applications. One major concern with these exempt products is that, during assembly or rework, lead-free components will have to be used due to the unavailability of tin-lead components. This will result in the mixing of tin-lead and lead-free metallurgies. The mixing of metallurgies can induce new reliability concerns. This study is focused on mixed solder joints formed by attaching lead-free components with tin-lead paste.

Solder interconnect reliability is influenced by the environmental imposed load, solder material properties and the microstructure formed between the solder and the metal surfaces to which the solder is bonded. Several lead-free metallurgies are being used for

component terminals, board pad plating and solder materials. These metallurgies react to form the microstructure of a solder joint. Microstructure of a solder joint continuously evolves and affects solder joint properties. A fundamental understanding on the microstructure is required to analyze the changes occurring in a solder joint with time and temperature and make predictions on solder joint reliability under thermal loading conditions.

This dissertation determines key microstructural features present in SnPb, lead-free and mixed solder joints. Changes in the microstructural features were determined for SnPb, lead-free and mixed solder joints exposed to isothermal aging conditions. The effect of microstructural changes on reliability was determined by conducting thermal fatigue reliability tests for SnPb and lead-free solder joints. Whereas, for mixed solder joints, hypotheses has been determined based on microstructural analysis on their thermal fatigue performance compared to SnPb joints. This dissertation doesn't include the effect of microstructural changes on the reliability of mixed solder joints. This dissertation doesn't include the reliability tests for mixed solder joints.

Two microstructural features namely, intermetallic compounds (IMC) and Pb phase were characterized for SnPb, lead-free and mixed solder joints. IMCs are formed at the solder to pad metallization interface and in the bulk solder. It was determined that reaction between Sn3.0Ag0.5Cu solder and Ni/Au component side metallization result in interfacial IMCs consisting of $Ni_3Sn_4$ IMC in the as-reflowed stage and IMCs such as $(NiCu)_3Sn_4$, $(Cu,Ni)_6Sn_5$ and $(Au,Ni)Sn_4$ after thermal aging of 350 hours at 125ºC. With pad metallization of ImAg, ImSn and OSP, IMCs such as $Cu_6Sn_5$ are formed after reflow followed by formation of a new $Cu_3Sn$ IMC phase after thermal aging of 350 hours at

125ºC. $Cu_6Sn_5$ and $Ag_3Sn$ IMC were found distributed in bulk solder joints in the as-reflowed and aged (125ºC for 100, 350 and 1000 hrs) solder joint.

This dissertation demonstrated that under thermal cycling, intergranular crack propagates between Sn grains in the bulk solder and $Cu_6Sn_5$ IMCs present at Sn grain boundaries in the bulk solder influence crack propagation. It was demonstrated that isothermal aging for 350 hrs at 125ºC causes coarsening of $Cu_6Sn_5$ IMC particles in the bulk solder which results in a 50% reduction in number of $Cu_6Sn_5$ IMC particles in the bulk solder, thus promoting the crack to propagate faster along the grain boundary. This dissertation determined that isothermal aging for 350 hrs at 125ºC would cause a 25% reduction in characteristic life for lead-free solder joints due to the changes associated with $Cu_6Sn_5$ IMC particles.

In conventional SnPb solder joints Pb phase present in the bulk solder coarsens as a function of time and temperature and influences thermal fatigue reliability. Due to the presence of Pb in mixed solder joint, this dissertation determined the extent of coarsening in mixed solder joints compared with SnPb joints. It was determined that mixed solder joints are not prone to Pb phase coarsening under aging for 350 hrs at 125ºC as opposed to SnPb solder joints and therefore would have better thermal fatigue performance compared to SnPb joint under these conditions. This dissertation demonstrated that the presence of Pb in mixed solder results in a 30 to 40% lower IMC thickness compared to Pb-free and SnPb solder joints by being present at the interface as a diffusion barrier between Ni and Sn for IMC formation. Presence of Pb has been known to act as diffusion barrier for SnPb solder joints.

# MICROSTRUCTURAL CHANGES UNDER ISOTHERMAL AGING AND THEIR INFLUENCE ON THERMAL FATIGUE RELIABILITY FOR TIN-LEAD AND LEAD-FREE SOLDER JOINTS, INCLUDING MICROSTRUCTURAL CHANGES UNDER ISOTHERMAL AGING IN MIXED SOLDER JOINTS

By

Anupam Choubey

Dissertation submitted to the Faculty of the Graduate School of the
University of Maryland, College Park, in partial fulfillment
of the requirements for the degree of
Doctor of Philosophy
2007

Advisory Committee:

Professor Michael G. Pecht, Chair
Professor Abhijit Dasgupta
Professor Manfred Wuttig
Associate Professor Peter Sandborn
Associate Professor Patrick McCluskey

**© Copyright by**
**Anupam Choubey**
**2007**

## Acknowledgment

First and foremost, I would like to express my deep sense of gratitude to Prof. Michael Pecht for having granted me this opportunity to work on this interesting topic and continuously challenging me to set a higher standard. I thank him for his continuous support towards the progress of this work and taking the time to review and guide me throughout the course of this study.

I would like to especially thank Dr. Michael Osterman and Dr. Sanka Ganesan for their excellent guidance, support and encouragement for this study. I am also thankful to Dr. Michael Osterman for including me in the Long term Lead-free Consortium, which helped me a lot towards the progress of this work. I am also thankful to Prof Abhijit Dasgupta, Prof. Patrick McCluskey, Prof. Peter Sandborn and Prof. Manfred Wuttig for their continued interest and efforts involved in reviewing my work.

I further extend my thanks to Dr. Diganta Das, Dr. Michael Azarian and Dr. Yu Hao for helping me provide technical guidance in my presentations and thesis. Comments from presentation greatly helped me guide through the progress of this work.

I would like to thank all my friends and colleagues, Sony Mathew, Dr. Keith Rogers, Dr. Sanjay Tiku, Dr. Nikhil Vichare, Dr. Reza Keimasi, Dr. Yan Liu, Dr. Dan Donahoe, Bo Song, Dr. Haiyu Qi, Dr. Tong Fang, Dr. Yuki Fukuda, Bhanu Sood, Anshul Shrivastava, Sachin Kumar, Dr. Ji Wu, Dr. Peter Rogers, Dr. Yuliang Deng, Dr. Sheng Zhan, Rajeev Mishra, Shirsho Sengupta, Snehanshu Chowdhary, Lyudmyla Panashchenko, Brian Tuchband, Jie Gu, Dr. Joe Varghese, Gayatri Cuddalorepatta, Yuxun Zhou for their invaluable inputs for this work.

Finally, I would like to extend very special thanks to my wife Ajita Mathur for her constant support and encouragement towards my work. I would like to thank my parents for standing by all my decision and constantly encouraging me towards my endeavors.

## Table of contents


List of Publications ........ vi

List of Figures ........ vii

List of Tables ........ xii

Chapter 1: INTRODUCTION ........ 1

1.1 Brief overview ........ 1

1.2. Mixed solder interconnects ........ 2

1.3. Problem statement ........ 3

1.4 Dissertation overview ........ 5

1.5 Asssumptions ........ 5

Chapter 2: LITERATURE REVIEW ........ 7

2.1. Studies on reliability for mixed solder joints ........ 8

2.2. Studies on microstructure and solidification behavior of mixed solder joints ........ 9

Chapter 3: INTERMETALLIC FORMATION ........ 13

3.1. Theory ........ 13

3.2. Design of experiment ........ 15

3.3. IMC thickness analysis ........ 18

3.4. Intermetallic composition analysis ........ 23

3.5. “So-called” Kirkendal Voids ........ 29

3.6. Conclusions ........ 33

Chapter 4: MICROSTRUCTURE OF MIXED SOLDER JOINTS ........ 36

4.1. Theory ........ 36

4.2. Experimental design ........ 37

4.3. Lead (Pb) phase distribution and coarsening ........ 38

4.4. Intermetallic compound thickness analysis ........ 43

4.5. Discussion and Summary ........ 49

Chapter 5: RELIABILITY TEST ........ 51

5.1. Theory ..... 51
5.2. Design of Experiment ..... 53
5.3. Reliability test results ..... 56
5.4. Physical microscopic analysis ..... 58
5.5. Conclusions ..... 70
Chapter 6: PULL STRENGTH TEST ..... 72
6.1. Theory ..... 72
6.2. Design of experiment ..... 72
6.3. Test results ..... 75
6.4. Conclusions ..... 84
CONTRIBUTIONS ..... 86
REFERENCES ..... 89

# List of Publications

- Choubey A., Menschow D., Ganesan S., and Pecht M., “Effect of Aging on Pull Strength of SnPb, SnAgCu and Mixed Solder Joints in Peripheral Surface Mount Components”, *Journal of SMTA*, Vol. 19, Issue 2, pp. 33-37, April 2006.
- Choubey A., Wu J., Ganesan S., and Pecht M., “Lead-Free Assemblies in High Temperature Applications”, *Proceeding of IMAPS International Conference on High Temperature Electronics (HITECH 2006)*, pp. 384-389, May 2006.
- Choubey A., Osterman M., Pecht M., and Hillman D., “Durability of Repaired and Aged Lead-free Electronic Assemblies”, *IPC Printed Circuits Expo, APEX, and Designers Summit*, Los Angeles, CA. Feb 18-22, 2007
- Choubey A., Osterman M., Pecht M., “Microstructure and Intermetallics Formation in SnAgCu BGA Components attached with SnPb Solder”, Accepted for Publication in *IEEE Transactions on Device and Materials Reliability*
- Choubey A., Osterman M. and Pecht M., “Durability of repaired and aged lead-free electronic assemblies”, *IEEE Transactions on Electronic Manufacturing*, Submitted for Review
- Choubey A., Osterman M. and Pecht M., “Effect of Isothermal Aging on the Reliability of Lead-free Solder Joints”, *IEEE Transactions on Component and Packaging Technologies*, Submitted for Review
- Choubey A., Wu J., Osterman M., Pecht M, Yun F., Yonghong Li, Ming Xu, "Evolution of intermetallics in Pb-free solder interconnects in BGA components with various lead and pad finishes”, *Journal of Electronic Materials*, Submitted for Review

## List of Figures

Figure 1: Pre-reflow stage for BGA attachment on board ................................................ 2

Figure 2: Post reflow stage of BGA attachment on board ................................................ 2

Figure 3: Pre-reflow stage for QFP attachment on board ................................................ 3

Figure 4: Post reflow stage of QFP attachment on board ................................................ 3

Figure 5: Printed circuit board with cut out features and BGA components .................... 17

Figure 6 : Interfacial IMC at the interface between copper pad on the board and solder. 18

Figure 7: Intermetallic growth – Sn3.0Ag0.5Cu and Sn37Pb Solder (Aged 125ºC)........ 19

Figure 8: Intermetallic growth – Sn3.0Ag0.5Cu Solder (Aged 100°C) .......................... 20

Figure 9: Intermetallic growth – Sn3.5Ag Solder (Aged 125°C) .................................... 21

Figure 10: Intermetallic growth – Sn3.5Ag Solder (Aged 100ºC) .................................. 21

Figure 11: Activation energies for IMCs formed with ENIG, ImAg and ImSn pad finishes ......................................................................................................................... 23

Figure 12: Sn3.0Ag0.5Cu joint with ImSn finish showing Cu6Sn5 and Cu3Sn IMC after aged at 125ºC for 350 hours ........................................................................ 24

Figure 13: Sn3.0Ag0.5Cu joint with ENIG finish showing (Cu, Ni)6Sn5 IMC and Ni(P), NiSnP layers– As-reflowed.......................................................................................... 24

Figure 14: Solder joint of BGA component with Sn3.0Ag0.5Cu solder attached with Sn3.0Ag0.5Cu solder on board pad with ImSn finish showing Ag3Sn IMC – As-reflowed ......................................................................................................................... 25

Figure 15: Needle like features in the microstructure of Sn3.0Ag0.5Cu solder (As-reflowed joint)........................................................................................................... 25

Figure 16: Magnified view of EDX analysis area from Figure 14 .................................. 26

Figure 17: Solder joint of BGA component with Sn3.0Ag0.5Cu solder attached with Sn3.0Ag0.5Cu solder on board pad with ENIG finish showing Ag3Sn IMC – As-reflowed ........................................................................................................................ 27

Figure 18: Solder joint of BGA component with Sn3.0Ag0.5Cu solder attached with Sn3.0Ag0.5Cu solder on board pad with OSP finish showing Ag3Sn IMC – Aged for 1000 hrs at 125ºC.......................................................................................................... 28

Figure 19: Needle type intermetallic layer for the as-reflowed joints ............................. 29

Figure 20: Planar intermetallics for the aged (125C for 350 hours) joints ...................... 29
Figure 21: Pad interface for ImSn finish (As-reflowed) with Sn3.0Ag0.5Cu solder joint31
Figure 22: Pad interface for ImSn finish (Aged 125°C for 350 hrs) with Sn3.0Ag0.5Cu solder joint ........................................................................................................ 31
Figure 23: Pad interface for ImSn finish (Aged 125°C for 1000 hrs) with Sn3.0Ag0.5Cu solder joint ........................................................................................................ 31
Figure 24: Pad interface for HASL finish (Aged 125°C for 350 hrs) with SnPb solder joint ........................................................................................................ 32
Figure 25: Pad interface ImAg pad finish - Sn3.0Ag0.5Cu solder joint (Aged 125°C for 350 hours) ........................................................................................................ 32
Figure 26: Black pad at the pad interface for ENIG- As-reflowed – Sn3.0Ag0.5Cu solder joint ........................................................................................................ 33
Figure 27: Black pad at the pad interface for ENIG- As-reflowed - Sn3.0Ag0.5Cu solder joint (Magnified view of pad interface) ........................................................ 33
Figure 28: Comparison of change in Pb phase area for mixed and SnPb solder joints due to aging........................................................................................................ 41
Figure 29: Distribution of Pb phase in mixed solder joint (non aged)............................ 42
Figure 30:Distribution of Pb phase in mixed solder joint aged (350 hours at 125 ºC)..... 42
Figure 31: Distribution of Pb phase in SnPb solder joint (Non aged) ............................ 42
Figure 32: Distribution of Pb phase in SnPb solder joint aged (350 hours at 125 ºC) ..... 42
Figure 33: SnPb solder joint – As reflowed.................................................................. 43
Figure 34: Mixed (SnAgCu BGA assembled with SnPb paste) solder joint - As reflowed ........................................................................................................ 43
Figure 35: Intermetallic growth for Pb-free and SnPb solder joints due to aging at 125 °C. ........................................................................................................ 45
Figure 36: Intermetallic growth for mixed solder joints (Sn3.0Ag0.5Cu solder balls attached with Sn37Pb solder) due to aging at 125 °C.................................................... 46
Figure 37: Segregation of Pb at the component side for mixed solder joint (Pb-free solder balls-SnPb solder paste)........................................................................................ 46
Figure 38: Segregation of Pb at the board side for mixed solder joint (Pb-free solder balls-SnPb solder paste)........................................................................................ 47

Figure 39: Sn3.0Ag0.5Cu solder joint on ImSn pad finish (aged at 125 °C for 350 hrs) showing IMC thickness ... 48
Figure 40: Mixed solder joint on ImSn pad finish (aged at 125 °C for 350 hrs) showing lower IMC thickness than Pb-free joint. ... 48
Figure 41: Reliability results indicating 25% reduction in characteristic life ($\eta$) of aged compared to non-aged lead-free joints ($\beta$ is the slope and $\rho$ is the correlation coefficient) ... 57
Figure 42: Reliability comparison of aged and non-aged SnPb solders joints showed no significant difference in characteristic life ... 57
Figure 43: Optical polarized image of as- reflowed Sn3.0Ag0.5Cu BGA joint showing tin grain colonies in the bulk solder (Grain colonies are marked by number 1 to 5) ... 60
Figure 44: Optical polarized image of Sn3.0Ag0.5Cu BGA joint aged at 125ºC for 350 hours showing tin grain colonies in the bulk solder (Grain colonies are marked by number 1 to 2) ... 60
Figure 45: SEM image showing grain colony boundary between tin grains 3 and 4 in Figure 43 ... 61
Figure 46: Presence of IMC in bulk solder of non-aged lead-free solder joint (Etched solder joint) ... 62
Figure 47: Presence of IMC in bulk solder of aged lead-free solder joint (Etched solder joint) ... 62
Figure 48: Number of IMC in the bulk solder for aged and non-aged solder joints ... 62
Figure 49: Image of tin grains near the cracked region in a lead-free solder joint after temperature cycling ... 64
Figure 50: Crack location for lead-free solder joint after thermal cycling. ... 65
Figure 51: Ion image from FIB showing crack location on the component side for lead-free solder joint (Image shows the presence of $Cu_6Sn_5$ IMC in the bulk solder) ... 66
Figure 52: Magnified ion image of crack path for lead-free solder joint ... 67
Figure 53: Electron microscopy image showing the crack path for lead-free solder joint (crack tends to follow the pattern by passing along the grain boundaries) ... 67
Figure 54: SEM image showing crack passing around the IMC in bulk solder ... 69

Figure 55: Ion beam image of thermal cycled solder joint with no aging prior to thermal cycling.......... 69
Figure 56: Printed circuit board.......... 73
Figure 57: Cutout QFP package assembly.......... 73
Figure 58: QFP package dimensions (mm).......... 73
Figure 59: Sample orientation schematic.......... 75
Figure 60: Effect of aging on pull strength for Sn3.0Ag0.5Cu solder with Sn lead finish with ENIG, ImSn, ImAg and OSP pad finish on FR4 board. Pull strength results are also shown for assemblies with SnPb lead finish attached with SnPb solder on HASL pad finish represented by HASL-SnPb.......... 76
Figure 61: Fracture surface on pad side for QFP (Sn) - Sn3.0Ag0.5Cu solder - ENIG pad finish sample, Aged at 125C for 350 hours where the elemental analysis was conducted77
Figure 62: Cross-sectional view of fracture surface for QFP (Sn) - Sn3.0Ag0.5Cu solder - ENIG pad finish sample, Aged at 125C for 350 hours – Fracture site found to be at the IMC.......... 78
Figure 63: Cross-sectional view of fracture surface for QFP (Sn) - Sn3.0Ag0.5Cu solder - ImAg pad finish sample, Aged at 125C for 350 hours – Fracture site between the lead and solder interface.......... 78
Figure 64: Effect of aging on pull strength for Sn3.0Ag0.5Cu solder with SnCu lead finish with ENIG, ImSn, ImAg and OSP pad finish on FR4 board.......... 79
Figure 65: Effect of aging on pull strength for Sn3.0Ag0.5Cu solder with SnBi lead finish with ENIG, ImSn, ImAg and OSP pad finish on FR4 board.......... 79
Figure 66: Effect of aging on pull strength for Sn3Ag0.5Cu solder on FR4 board.......... 81
Figure 67: Effect of pad finish on pull strength for Sn3Ag0.5Cu solder on FR4 board... 82
Figure 68: Effect of lead finish on pull strength for Sn3Ag0.5Cu solder on FR4 board.. 82
Figure 69: Effect of aging on pull strength for Mixed - SnPb (Pb-free QFP- SnPb paste), Pure Pb-free (Pb-free QFP- Sn3Ag0.5Cu paste) and Pure SnPb (SnPb QFP- SnPb paste) assemblies.......... 83
Figure 70: Effect of pad finish on pull strength for Mixed –SnPb (Pb-free QFP- SnPb paste), Pure Pb-free (Pb-free QFP- Sn3Ag0.5Cu paste).......... 84

Figure 71: Effect of lead finish on pull strength for Mixed –SnPb (Pb-free QFP- SnPb paste), Pure Pb-free (Pb-free QFP- Sn3Ag0.5Cu paste).................................................. 84

## List of Tables

Table 1: Literature summary of lead-free components attached with SnPb solder 11

Table 2: Effect of metallurgy on the behavior of mixed solder interconnect (Ingot samples) 12

Table 3: Test sample matrix 16

Table 4: Results of composition analysis conducted on a point from Figure 16 27

Table 5: Circuit board solder and pad finish assembly matrix 38

Table 6: Composition of phase at last solidification temperature (181°C) for Sn-Cu-Pb system 39

Table 7: Type of IMCs for Several Pad Finishes 47

Table 8: Board assembly matrix 55

Table 9: Interconnect assembly configuration – FR4 boards 74

Table 10: Interconnect assembly configuration - PI boards 74

Table 11: Atomic % of elements at the fracture surface for QFP(Sn) - Sn3.0Ag0.5Cu Solder - Aged at 125ºC for 350 hrs for pad with ImAg and ENIG finish 77

# Chapter 1: INTRODUCTION

## 1.1 Brief overview

For several years, the reliability of lead-free solder interconnects has been the subject of intense investigation. The research has been driven by government legislation and market pressures to eliminate lead from electronic hardware. Most electronics companies have transitioned to Pb-free processes, both to comply with government legislation and to avoid issues related to mixing of SnPb and Pb-free metallurgies[1]-[5]. However, exemptions from Pb-free legislation have been granted for certain products, especially those intended for high-reliability applications. An overview of exemptions from Pb-free legislation can be found in [1]-[5] . One major concern with these exempt products is that, during assembly or rework, Pb-free components will have to be used due to the unavailability of SnPb components. This will result in the mixing of SnPb and Pb-free metallurgies.

The mixing of metallurgies can induce new reliability concerns, because solder joint reliability depends on mettalurgies which make up the microstructure of the solder joint, which influence the reliability. Furthermore, the microstructure of a solder joint continues to evolve over time depending on temperature and other loading conditions. Though, the industry is gaining confidence in the use of lead-free process with respect to manufacturing yields and reliability, mixing of Pb has become a topic of recent concern.

### 1.2. Mixed solder interconnects

A solder joint formed due to the mixing of SnPb and Pb-free material is termed a "mixed solder joint". Typical area array lead-free component solder ball is a combination of Sn, Ag and Cu with the Ag content varying from 3.0 to 4.0 weight%, Cu content by 0.5 to 0.7 weight% and the balance made up by Sn. For ball grid array (BGA) component mixing may occur when a BGA with Pb-free solder ball is attached with SnPb solder paste. Figure 1, shows the pre-reflow stage, wherein the solder paste is printed on the board followed by BGA placement. Figure 2 shows the post-reflow stage, wherein the solder ball mixes with the paste to form a solder joint.

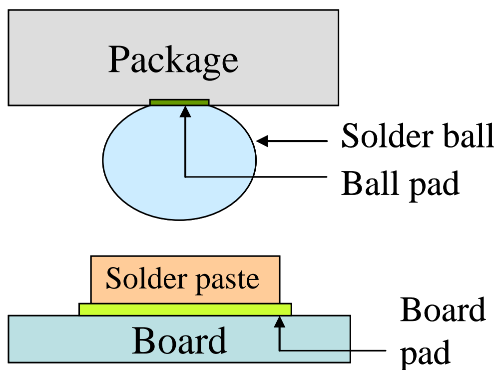


**Figure 1: Pre-reflow stage for BGA attachment on board**

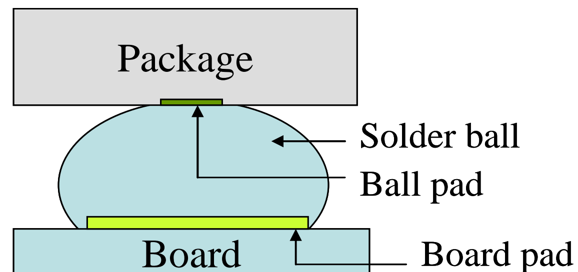


**Figure 2: Post reflow stage of BGA attachment on board**

Typical peripheral leaded lead-free components are coated with Sn, SnCu or SnBi lead finishes. Mixing of Pb occurs during the assembly or rework of components with Pb-free terminal using SnPb paste. Figure 3 shows the pre-reflow stage for a quad flat pack (QFP) component; where in the solder paste is printed on the board followed by QFP placement. Figure 4 shows the post-reflow stage in which the solder joint is formed by the attachment between the metallurgy on the lead and the solder paste. Due to the Pb-

free transition various lead-free board pad finishes are being used by industry such as Immersion Ag (ImAg), Immersion Sn (ImSn), Immersion Au over Electroless Ni (ENIG) and Organic solderability preservative (OSP) finish. The reaction between these Pb-free metallurgies with SnPb solders also play a key role on the reliability of solder joints.

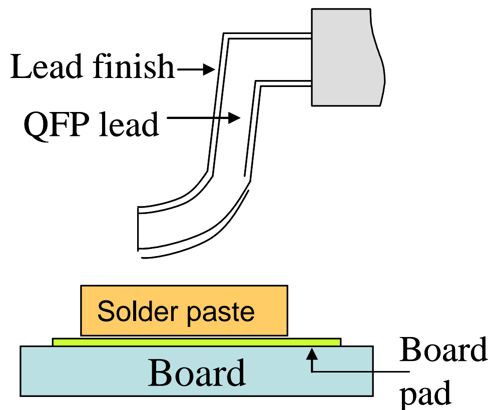


**Figure 3: Pre-reflow stage for QFP attachment on board**

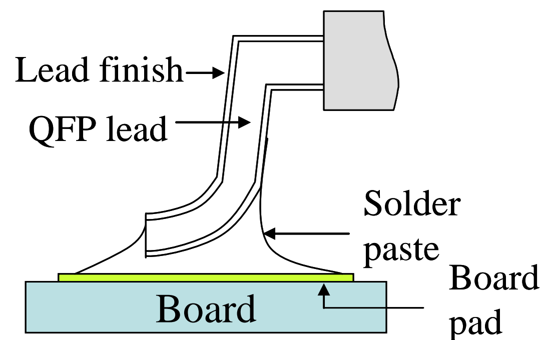


**Figure 4: Post reflow stage of QFP attachment on board**

### 1.3. Problem statement

Solder joint reliability depends on the changes those occur in its microstructure due to loading conditions. Microstructure plays a key role in influencing the time to failure for solder joints. Several studies have been conducted to investigate the reliability of solder joints subjected to several loading conditions and material combinations and are discussed in Chapter 2. To arrive at a fundamental understanding of reliability, there is a need to analyze the microstructural changes that occur as a function of time and temperature for Pb-free and mixed solder joints. This study examines the microstructure of Pb-free solder joints and mixed solder joints formed by attaching ball grid array (BGA) components having lead-free solder balls with SnPb solder paste.

Two aspects of solder joint microstructure were examined which included the study of Pb phase distribution in mixed solder joints and the growth on intermetallic compounds in Pb-free and mixed solder joints. It has been reported in the literature that the Pb phase has a tendency to coarsen depending on time, temperature and stress which affect the thermal fatigue life for SnPb solders [6, 7]. Coarsening is a structural change where the average size of particles in a microstructure increases with time. As the amount of coarsening relates to the solder degradation, coarsening of Pb phase was studied for mixed solder joints to examine the amount of degradation of mixed solder joints compared to conventional SnPb joints.

Another microstructural feature are the intermetallic compounds (IMC) which are formed during the soldering process, when the solder is in molten state due to the interdiffusion of two or more metals. These intermetallics then continue to grow due to aging and have been well known to influence the reliability of solder joints. In this study, the growth of intermetallics has been examined due to the presence of Pb in mixed solder joints.

To study the influence of these microstructural changes, a reliability study was conducted. This study reports a correlation between the microstructural changes in solder joint due to time and temperature and their influence on reliability of solder joints. As microstructural changes occur due to time and temperature, solder joints were exposed to thermal cycling loading. It's known that QFP component take a longer time to fail in thermal fatigue compared to BGA components. Therefore only BGA components were exposed to thermal cycling whereas pull test was conducted on the leads of QFP components to assess the strength of solder joints on exposure to time and temperature.

### 1.4 Dissertation overview

This study investigates the microstructure of solder joints and the influence of changes in microstructural features on the reliability of surface mount components. First two chapters discuss about the microstructural features followed by results of reliability study conducted to analyze the effect of microstructural features on reliability. Chapter two discusses the studies and findings from previous published data on mixed solder joints. Chapter three discusses intermetallic compounds, one of the key microstructural features which influence the reliability followed by chapter four which discusses changes in Pb phase, another microstructural feature, reported to influence solder joint reliability. Microstructural studies are followed by reliability study on BGA components in chapter five and pull strength study for QFP components in chapter six.

### 1.5 Asssumptions

From a manufacturing perspective mixed solder assemblies have a narrow window for the reflow temperature because of different melting temperatures of SnPb and Pb-free solders and the changes in solder volume depending on application. Due to the sensitivity to the mixing of Pb in the solder joints, process development should be conducted to develop a reflow process which would result in a homogeneous distribution of Pb over the entire solder ball. Assembly process for mixed solder joint was conducted in a high volume manufacturing facility with a developed reflow profile and was considered as a typical profile for mixed solder joints.

Solder joint geometry was considered to be consistent for the assemblies under analysis, over 100 solder balls were cross-sectioned to get a confidence on the geometry.

Several pad finishes are available in the industry such as ENIG, ImAg, ImSn and OSP. The quality of finish may depend on the plating process. Printed circuit boards were plated in a high volume manufacturing facility with a developed plating process. Plating process was considered typical for the individual finish under analysis.

Incomplete mixing of Pb has been reported to cause early failure of mixed solder joints. Mixing is found to be homogeneous and was also verified using SEM analysis for over 50 solder balls. Pb was found distributed over the entire solder joint for all the pad finish and solder combinations.

# Chapter 2: LITERATURE REVIEW

Various studies have been conducted on testing the reliability of mixed solder joints under various stress loading conditions and for various metallurgical combinations. In this section a summary of the studies conducted on mixed solders is discussed.

Table 1 provides summary and key findings from various studies on the assemblies prepared by attaching lead-free components with SnPb solder paste. Table 2 provides key findings of studies those have analyzed the solidification behavior of mixed solder interconnects and have assessed the reliability and strength of solder joints formed by varying the Pb percentage in the joint.

### 2.1. Studies on reliability for mixed solder joints

Studies [11][12] have reported the effect of reflow peak temperature on the reliability of the mixed solder joint (lead-free component-SnPb paste). They observed that insufficient melting of the solder ball with peak reflow temperature below the melting point of lead-free solder results in early failures in thermal cycling (500 cycles [11], 276 cycles [12]) whereas when the temperature is above the lead-free melting temperature solder joint reliability is comparable to pure SnPb and lead-free assemblies for area array components. Grossman et. al. [13] studied the reflow with peak reflow temperatures ranging from 210ºC to 245ºC. They observed insufficient melting of solder balls below 210ºC and excessive void formation with peak reflow temperature greater than 233ºC.

Studies conducted on thermal cycling reliability have reported that the fatigue life for mixed solder joints depends on component type [1] and pad finishes [11]. Hua et.al. [11], concluded that the assemblies on OSP pad finish perform better than ENIG in thermal cycling and drop tests.

Chalco et. al. [14] observed that the fatigue life of mixed solder assemblies for flip chip ball grid array (FCBGA) is equal to lead-free and for CSP equal to SnPb. Nelson

D. et. al. [16], reported the reliability under thermal cycling of Sn3.8Ag0.7Cu solder balls attached with Sn37Pb for flexBGA and tape ball grid array (TABGA). Thermal cycling data for flexBGA lead-free balls-SnPb solder paste attached systems show 10 % higher cycles to failure than pure lead-free assemblies. In TABGA, lead-free balls-SnPb solder paste attached assemblies show 20% decrease in cycles to failure than pure lead-free assemblies. Motorola [1] reported the thermal cycle test results for plastic ball grid array (PBGA) (Sn3.5Ag0.75Cu) assembled with SnPb solder. From this study it was observed that fatigue life of mixed solder assembly is 17 % greater than pure lead-free.

### 2.2. Studies on microstructure and solidification behavior of mixed solder joints

Further studies have been conducted to study the effect of Pb in mixed solder interconnect. Chung [17] mixed Sn4.5Ag0.5Cu solder with 3 % Sn37Pb solder and observed 2 peaks in Differential Scanning Calorimeter (DSC) analysis one at 181ºC and other at 218ºC which corresponds to 2 melting temperatures. The 2 melting temperatures observed are due to the dissolution of Pb in the solder matrix that results in the formation of a low melting phase (SnPbAg) that melts at 181ºC. In this study ball grid array (BGA) components with Sn4.5Ag0.5Cu solder balls were assembled with Sn37Pb paste. It was observed that Pb is finely distributed as a Pb rich phase where reflow temperatures are higher than lead-free melting temperatures. Researchers have also reported that due to the presence of Pb greater than 3%, solidification occurs over a wider temperature range from 220 ºC to 176 ºC as opposed to eutectic [17]-[20], though the significance of this solidification behavior on reliability has not been established.

Oliver [21] reported that the Pb phases after soldering were observed to exist mainly between the Sn dendrites. For lead-free components attached on SnPb finish they observed microcracks after 500 cycles during temperature cycling (-15 ºC to 125 ºC). Microcracks were observed passing through Pb phases that exist in Sn grain boundaries. For shear stress testing they varied 1, 2, 5, 10, 15, 20 wt% Pb contamination in the solder. By testing they observed that least reliable lead-free joints lie in the 2 % to 5 % Pb contamination region. For Pb contamination between 10 % and 15 % the reliability increases again and for 20 % Pb the contaminated joint performs better than pure lead-free joints. Zhu [22] studied the shear strength of mixed solder joints for 1206 capacitor. Two solders Sn3.5Ag and Sn5.0Sb were mixed with 5, 10, 15, 20 weight % of Sn37Pb solder. The shear force for solder joints without Pb contamination was about 15 % higher than for those with Pb contamination when shear test was performed at 125°C whereas no change in shear strength was observed in room temperature testing.

**Table 1: Literature summary of lead-free components attached with SnPb solder**

| Ref | Package | Pad finish /Solder ball | Test conditions | Findings |
|---|---|---|---|---|
| [11] | Stacked chip scale package (SCSP), very fine ball grid array (VFBGA) | ENIG, OSP /Sn4.0Ag0.5Cu ball | Thermal cycling (-40 ºC to 125 ºC), Drop testing (board mounted on fixture and dropped from a height of 1.5 m) | • Reflow at 208 °C < 217 °C (Lead-free melting) show failures at 500 cycles<br>• Failure rate > 5 % for SnPb control and < 5 % for Lead-free control and mixed after 800 cycles with reflow at 222 °C for both finish<br>• Drops to failure for mixed > SnPb and Lead-free for OSP finish for both component types<br>• Drops to failure for mixed < SnPb and Lead-free for ENIG for both component types |
| [12] | BGA | ENIG /Sn4.0Ag0.5Cu ball | Thermal cycle (–55 ºC to 125 ºC) | • Reflow (215 ºC) < Lead-free melting<br>• Average cycles to failure: 276 |
| [14] | FCBGA (14x22 mm) and CSP (7x6.5 mm) | OSP /Sn3.3Ag0.7Cu ball | Thermal cycle (0 ºC to 100 ºC) | • The fatigue life of mixed solder joint is comparable to pure SnPb in case of FCBGA and comparable to pure Lead-free for CSP assemblies. |
| [16] | TABGA, flexBGA | ENIG /Sn3.8Ag0.7Cu ball | Thermal cycle (–55 ºC to 125 ºC) | • In flexBGA, mixed assembly shows 10% higher cycles to failure than pure lead-free system.<br>• In Tape Array BGA, mixed assembly shows 20% lower cycles to failure than pure lead-free. |
| [1] | PBGA | Not reported /Sn3.5Ag0.75Cu ball | Thermal cycling (-40 ºC to 125 ºC) | Cycles to failure<br>• Mixed 17% > Lead-free<br>• Lead-free 23% > SnPb |
| [23] | PBGA, CBGA | OSP, ImAg /Sn3.0Ag0.5Cu ball Sn4.0Ag0.5Cu ball | Thermal cycling (0 ºC to 100 ºC) | PBGA and CBGA reliability for Mixed interconnect are comparable with pure SnPb assemblies |
| [22] | 1206 leadless capacitors | Mixed solders Sn3.5Ag and Sn0.5Sb with 5-20% Sn37Pb | Shear test at room temperature and 125 °C | • Pb observed in SnAg grain boundaries.<br>• 15% reduction in shear force observed with Pb contamination |

| Ref | Package | Pad finish /Solder ball | Test conditions | Findings |
|---|---|---|---|---|
| | | paste | | at 125 °C |
| [13] | BGA | Sn3.8Ag0.7Cu ball | Reflow at 210 - 246 °C | • Insufficient melting at 210°C<br>• Void formation observed at 233°C |

**Table 2: Effect of metallurgy on the behavior of mixed solder interconnect (Ingot samples)**

| Ref | Package | Solder material | Test conditions | Findings |
|---|---|---|---|---|
| [24] | Test specime n as per the standard | Sn4Ag0.5Cu mixed with 0.5% and 1% Pb | ASTM E606 fatigue testing | • Cycles to failure reduced to 50% with 0.5% Pb and 75% with 1% Pb |
| [21] | Test fixture designed | Sn3.5Ag0.7Cu solder mixed with 1,2,5,10,15,20 weight % Pb | Ring and pin test | • Joint with 20 % Pb was 40 % more reliable than pure lead-free and with 5% Pb showed 70% lower reliability than pure Lead-free |
| [18] | Alloy paste | Sn3.8Ag0.7Cu mixed with 10 % SnPb | DSC to study melting temp. | • Solidification starts at 220 and last liquid solidifies at 176 °C |
| [17] | Alloy paste | Sn4.5Ag0.5Cu components with 3% SnPb | DSC to study the melting temp. | • Two melting points observed 181°C and 218°C. Lead-free solders melt at 217°C where as SnPb solders melt at 183°C. The temperature of 181°C was found due to the formation of low melting phase (SnPbAg) due to the dissolution of Pb in Lead-free solder. |

# Chapter 3: INTERMETALLIC FORMATION

## 3.1. Theory

In a surface mount electronic assembly, interconnections are made by attaching component terminals with a solder material onto a printed circuit board (PCB). The attachment process involves the interaction of metallurgies from the component terminals, solder paste and finishes on the base metal of PCB. Component terminal metallurgies include finishes on the leadframe for peripheral leaded component (e.g., QFPs) such as matte tin (Sn), tin copper (SnCu) and tin bismuth (SnBi) whereas solder ball material for ball grid array (BGA) component such as an alloy of Sn-3~4%Ag-0.5~2%Cu (SAC).

Tin-silver-copper alloys have become the mainstream lead-free alloys for electronics assembly. NEMI, JEITA, International Tin Research Institute (ITRI) and the European Department of Trade and Industry (DTI) have recommended various compositions of this alloy. There are numbers of variations in the composition of the alloy, among which the most characterized alloy composition is Sn-3~4Ag-0.5~2Cu.

For printed circuit boards, copper is used to form solderable mounting points for electronic devices and interconnects between devices. Although copper can have good solderability, it oxidizes quickly when exposed to the environment conditions causing reduced wettability and solderability. Surface finishes are commonly used to protect the copper metallization of the PCB from oxidation, as well as contaminants and mishandling prior to assembly. Surface finish options typically used in the industry include immersion-gold over electroless or electrolytic nickel (ENIG), organic solderability

preservative (OSP), immersion tin (ImSn), immersion silver (ImAg) as well as lead-free (SAC or SnCu) Hot Air Solder Leveling (HASL).

Metal component terminals and board pad finishes react and form compounds with solder, called as intermetallic compounds (IMCs). Initial formation of intermetallic compounds is governed by dissolution process. Dissolution is the chemical change that takes place as solid materials melt into liquid materials. Dissolution of solder with metal substrate and their finishes occur during the soldering process to form intermetallics. Once the intermetallics are formed, their growth is governed by a thermally activated diffusion process. The initial formation of intermetallic compounds (IMC) during soldering ensures a good metallurgical bond, but the growth of these IMCs results in a weak interface that would lead to failure. Studies have reported that intermetallic compounds (IMC) formed at the interface between the base metal and the solder, influence reliability [29][30].

Several studies have been conducted to investigate the formation of intermetallics for Pb-free solder connections. Zheng *et al* [31] studied the formation of IMC at the interface between various board pad finishes such as ImSn, ImAg, OSP and ENIG for Sn3.8Ag0.7Cu solder joints. They found that the pad finish material influences the growth and composition of IMC formed at the interface. They also concluded that the growth of IMC does not have any influence on the shear strength of solder joints as all the failures were found in the bulk solder rather than in the interfacial IMC. Several other studies [31][32][33] have investigated the IMC thickness under various loading conditions such as thermal shock, thermal cycling and isothermal aging with specific pad

finishes. As industry is narrowing down to Sn3.0Ag0.5Cu and Sn3.5Ag solder, there is need to understand its interaction with copper pad metallization.

This study evaluates the effects of isothermal aging (125ºC and 100ºC), solder, and pad finish on the growth and composition of interfacial intermetallics. BGA components with Sn3.0Ag0.5Cu solder balls were assembled using either Sn3.0Ag0.5Cu or Sn3.5Ag solder. PCB finishes included ImSn, ImAg, ENIG and OSP. For comparison, intermetallic growth in solder joints of BGA components with Sn37Pb solder balls attached with Sn37Pb solder on HASL (SnPb) pad finish were examined.

### 3.2. Design of experiment

In this study, solder joints of BGA components were used to investigate intermetallic growth between solder and PCB copper pads. The BGAs were part of a common test vehicle being used in a larger lead-free reliability study. A photo of an assembled test specimen is provided in Figure 5. The BGA component had 256 Sn3.0Ag0.5Cu solder balls with 1mm pitch. The printed circuit boards were constructed of polyimide laminates and included ENIG, ImAg, ImSn or OSP pad finishes. Test specimens were assembled in a volume surface mount reflow operation using either Sn3.5Ag or Sn3.0Ag0.5Cu no-clean solders. Test sample matrix is shown in Table 3. Lead-free reflow was conducted at a peak reflow temperature of 246C with time above liquidus of 78 seconds. The assembled BGAs were detached using cut-out features built in the boards (see Figure 6). Detachment was done using dremel tool by cutting the board regions containing BGA components at four corners. Cut out features were designed to allow removal of specific board regions without cutting the whole board and disturbing

adjacent board regions. A set of cut out BGAs were subjected to thermal aging. Aging conditions included 100ºC and 125ºC for 350 and 1000 hours to accelerate the formation of intermetallics. One as-reflowed BGA component was also analyzed as a control to compare the IMC thickness before and after aging for each pad finish.

Table 3: Test sample matrix

| Solder paste | Solder ball | Pad finish | Aging conditions | Sample |
|---|---|---|---|---|
| SnPb | Sn37Pb | HASL (SnPb) | As-reflowed, 350 and 1000 hours at 125ºC and 100ºC | 1 BGA per each pad finish, solder paste and aging condition combination |
| Sn3.0Ag0.5Cu | Sn3.0Ag0.5Cu | ENIG, ImSn, ImAg, OSP | | |
| Sn3.5Ag | Sn3.0Ag0.5Cu | ENIG, ImSn, ImAg | | |

Specimens were mounted in a clear epoxy potting compound, cross-sectioned and polished to prepare for the IMC thickness measurements. Photos of solder joint cross-sections were taken using optical microscope. A polarized light source was used to facilitate identification of the IMC layer. IMC thickness measurements taken on optical images were verified using scanning electron microscope (SEM). Three solder joints per sample were analyzed and three measurements were taken per solder joint resulting in

nine readings per material combination. Mean and standard deviation based on these nine reading were utilized to compare thicknesses for various material combinations. Figure 6 is a cross section of solder to copper interface on pcb side showing the interfacial IMC formed for Sn3.0Ag0.5Cu solder assembly.

Figure 5: Printed circuit board with cut out features and BGA components

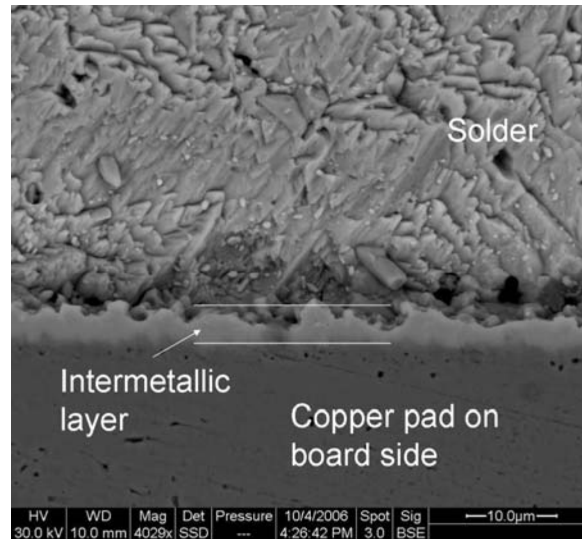


Figure 6 : Interfacial IMC at the interface between copper pad on the board and solder

### 3.3. IMC thickness analysis

IMC thickness for various pad finishes as a function of aging condition for Sn3.0Ag0.5Cu and Sn37Pb solder is presented in Figure 7. It was observed that after 350 hours of aging at 125°C, the IMC growth on ImSn, ImAg and OSP finishes were comparable, mean thickness of 2.5 to 3.5 µm was observed. The initial thickness of ENIG was lower than other finishes.

After 1000 hours of aging at 125°C similar trend were observed for pad finishes, mean IMC thickness was approximately 3 to 4 µm for ImSn, ImAg and OSP finishes, whereas for ENIG average IMC thickness was 2.8 ± 0.36 µm. Lower IMC thickness for ENIG pad finish is due a low reaction rate of nickel with tin at high temperatures.

For SnPb solder joints, an IMC thickness of 3.3 ± 0.22 µm was found after 1000 hours of aging at 125C which is lower than Pb-free solder joints Lower thickness for SnPb solder is attributed to the amount of tin in the solder. Pb-free solder contains 96.5 weight percent tin whereas tin-lead solder contains 63.0 weight percent tin. Amount of tin

governs the reaction with copper base metal and diffusion continues until the equilibrium is established at the solder to copper interface.

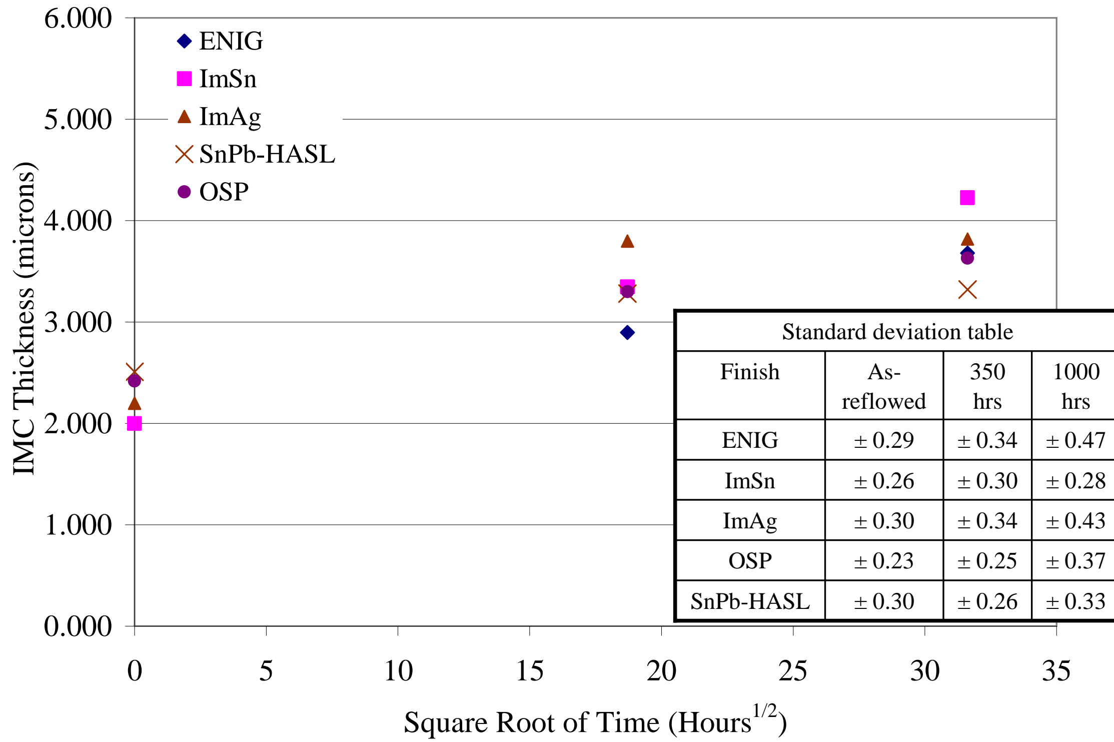


| Standard deviation table | | | |
|---|---|---|---|
| Finish | As-reflowed | 350 hrs | 1000 hrs |
| ENIG | ± 0.29 | ± 0.34 | ± 0.47 |
| ImSn | ± 0.26 | ± 0.30 | ± 0.28 |
| ImAg | ± 0.30 | ± 0.34 | ± 0.43 |
| OSP | ± 0.23 | ± 0.25 | ± 0.37 |
| SnPb-HASL | ± 0.30 | ± 0.26 | ± 0.33 |

Figure 7: Intermetallic growth – Sn3.0Ag0.5Cu and Sn37Pb Solder (Aged 125ºC)

Figure 8 shows the IMC thickness for samples exposed to aging at 100°C, it was observed that after 350 hours of aging, the IMC growth on ImSn, ImAg, and ENIG finishes was comparable, a thickness of 2.5 to 3 µm was observed. After 1000 hours of aging at 100°C, the IMC thickness was approximately 3 µm which is 1 µm less than IMC thickness at 125°C for 1000 hours aged joints.

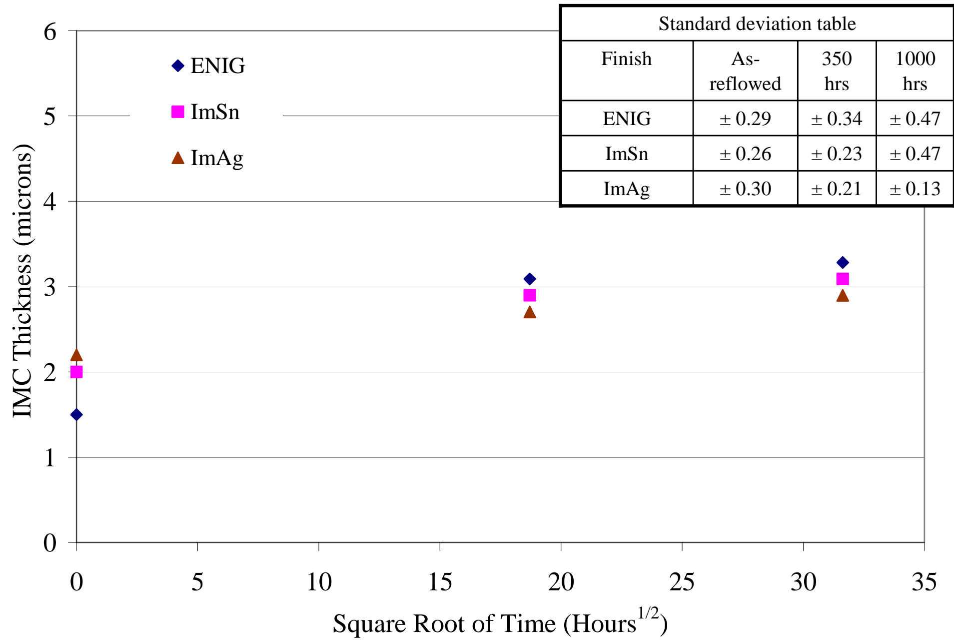


Standard deviation table

| Finish | As-reflowed | 350 hrs | 1000 hrs |
|---|---|---|---|
| ENIG | ± 0.29 | ± 0.34 | ± 0.47 |
| ImSn | ± 0.26 | ± 0.23 | ± 0.47 |
| ImAg | ± 0.30 | ± 0.21 | ± 0.13 |

Figure 8: Intermetallic growth – Sn3.0Ag0.5Cu Solder (Aged 100°C)

Figure 9 shows the IMC thickness for various pad finishes for Sn3.5Ag solder for aging condition of 125ºC and Figure 10 shows the IMC thickness for various pad finishes for Sn3.5Ag solder for aging condition of 100ºC. It was observed that IMC thickness with the Sn3.5Ag solder had a greater range of values that varied according to type of pad finish. The thickness range was 1.5 to 4.5 µm after 350 hrs of aging and 2.2 to 4.5 µm after 1000 hrs of aging. For both Sn3.0Ag0.5Cu and Sn3.5Ag solders, ENIG pad finish resulted in a thinner IMC layer.

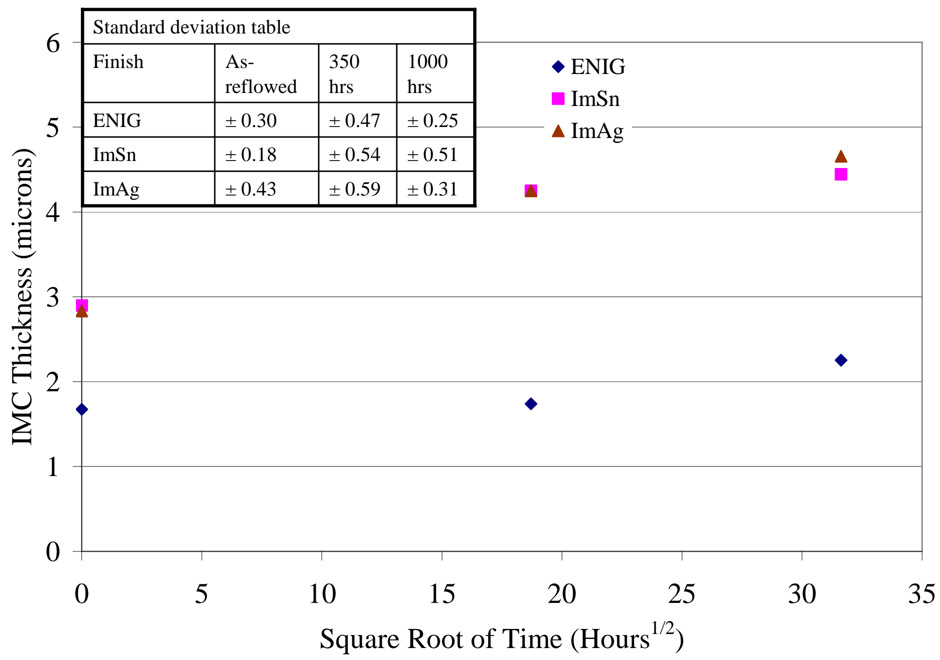


Figure 9: Intermetallic growth – Sn3.5Ag Solder (Aged 125°C)

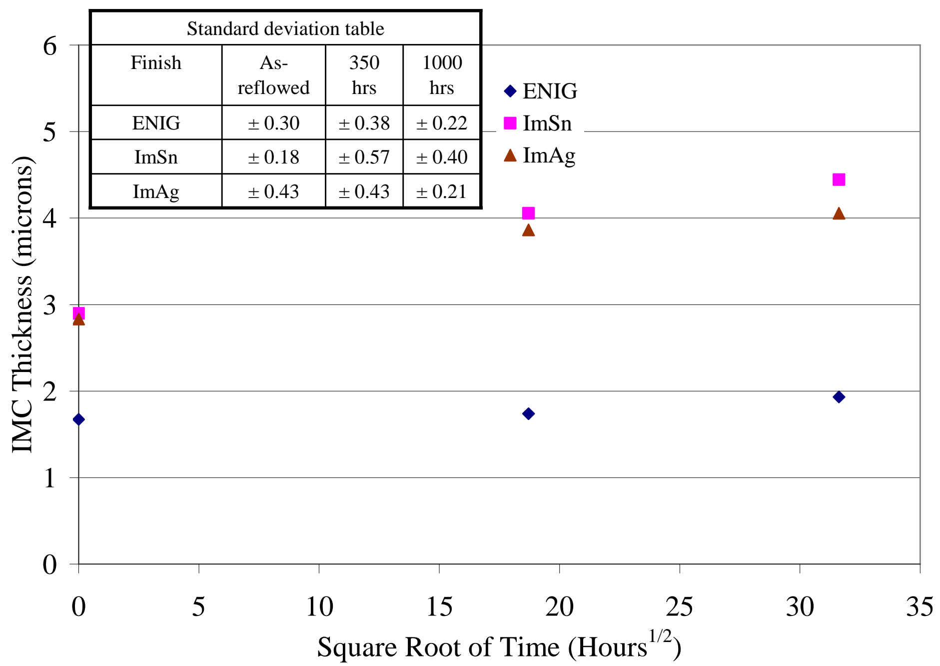


Figure 10: Intermetallic growth – Sn3.5Ag Solder (Aged 100ºC)

The growth rate at each temperature was calculated by taking square of the slope obtained from the least square linear regression of average thickness (d- d0), against the square root of time, t.

$$d = d_0 + \sqrt{Dt} \qquad (1)$$

Where, d is the IMC layer thickness at time t, d0 is the IMC layer thickness in the as-reflowed condition, D is growth rate for each temperature 100ºC and 125 ºC.

An arrhenious relationship (see equation 2) was then used to calculate the effect of temperature on the growth rate. The activation energy was calculated from the slope of ln (D) and 1/KT (see Figure 11), where K is the Boltzmann constant (8.617 e-5 electron Volts/Kelvin), T is the temperature at which the test was conducted, 100ºC and 125 ºC in this study.

$$D = D_0 \exp(-\frac{Q}{KT}) \qquad (2)$$

$$Ln(D) = Ln(D_0) + (-\frac{Q}{KT}) \qquad (3)$$

Activation energy for ENIG, ImSn and ImAg with Sn3.0Ag0.5Cu solder was found to be 0.54 ± 0.1 eV, 0.91 ± 0.12 eV and 1.03 ± 0.1 eV respectively (see Figure 11). Activation energies were calculated considering the combined effect of all the IMCs present at the interface. Activation energies for Sn-Ag-Cu based solders have been previously reported to be between 0.25 eV to 1.05eV and for SnPb to be 0.94 eV [31][32][33].

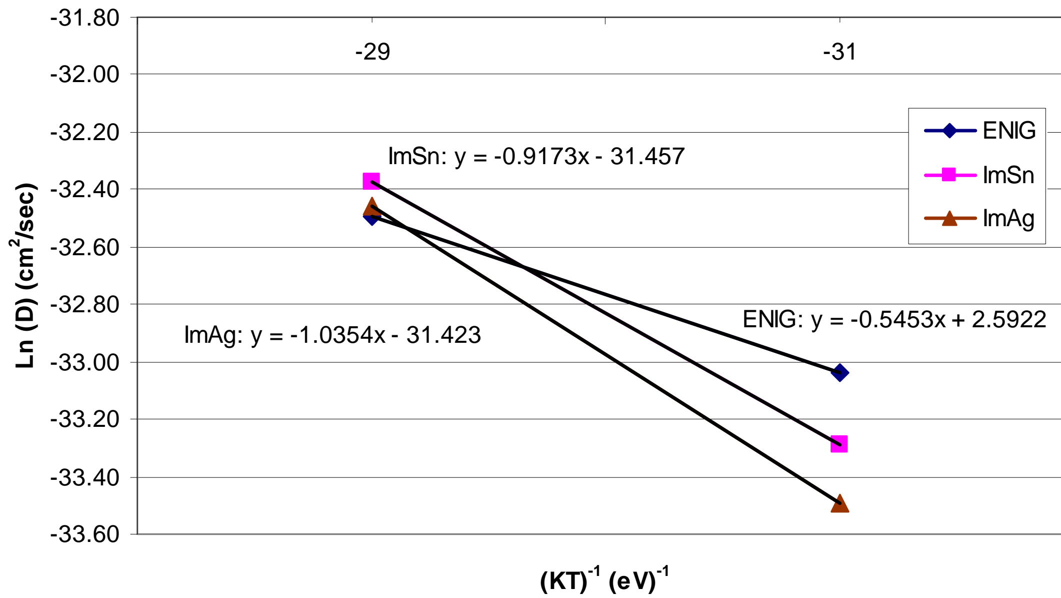


Figure 11: Activation energies for IMCs formed with ENIG, ImAg and ImSn pad finishes

## 3.4. Intermetallic composition analysis

Figure 12 shows the presence of Cu6Sn5 and Cu3Sn in the as-reflowed solder joint assembled on boards with the ImSn pad finish. After 100 hours of aging at 125ºC, Cu3Sn IMCs were found between Cu6Sn5 and the copper pad for boards with ImSn and ImAg pad finish.

At the interface between solder and copper pads with ENIG pad finish, depicted in Figure 13, (Cu,Ni)6Sn5 intermetallics were found For the ENIG pad, Nickel (Ni) with Phosphorus, Ni(P), was observed immediately above the copper followed by NiSnP. The source of phosphorus comes from the electroless Ni plating method, where Ni is deposited as a mixture of Ni and Nickel-Phosphorus (Ni-P).

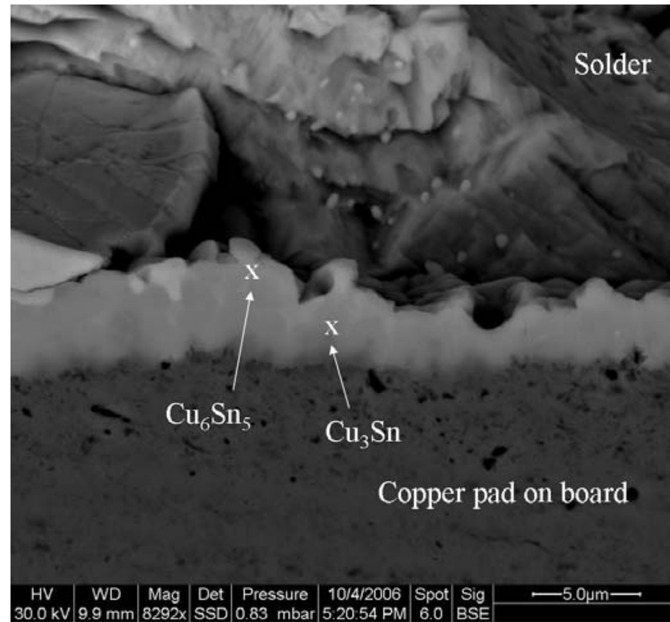


Figure 12: Sn3.0Ag0.5Cu joint with ImSn finish showing Cu6Sn5 and Cu3Sn IMC after aged at 125ºC for 350 hours

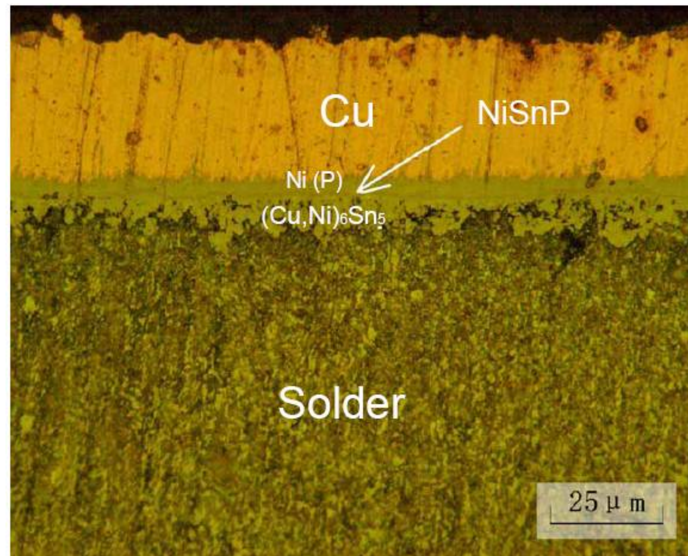


Figure 13: Sn3.0Ag0.5Cu joint with ENIG finish showing (Cu, Ni)6Sn5 IMC and Ni(P), NiSnP layers– As-reflowed

Figure 14 shows an as-reflowed solder joint of a BGA component with Sn3.0Ag0.5Cu solder balls attached with Sn3.0Ag0.5Cu solder. Needle like features were observed in the bulk solder and at solder to copper interface, these features were observed

to be present either in groups or as single entity and were found distributed over the entire solder ball (see Figure 15). Element analysis using energy dispersive X-ray technique in ESEM found the needle structures to be rich in silver (Ag) –tin (Sn) intermetallics.

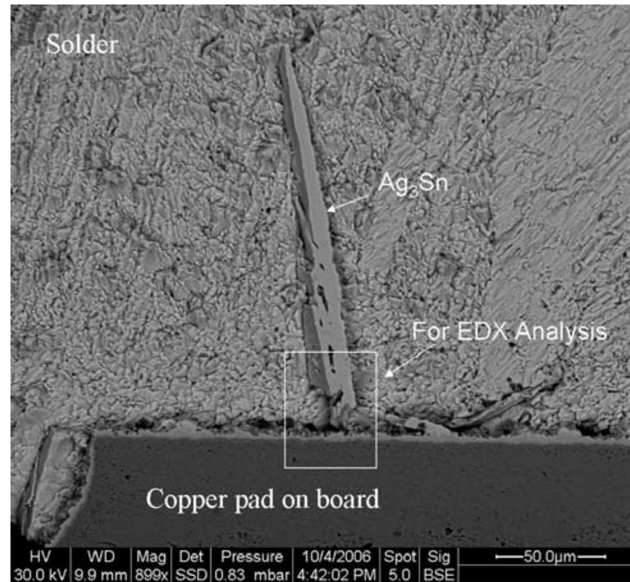


Figure 14: Solder joint of BGA component with Sn3.0Ag0.5Cu solder attached with Sn3.0Ag0.5Cu solder on board pad with ImSn finish showing Ag3Sn IMC – As-reflowed

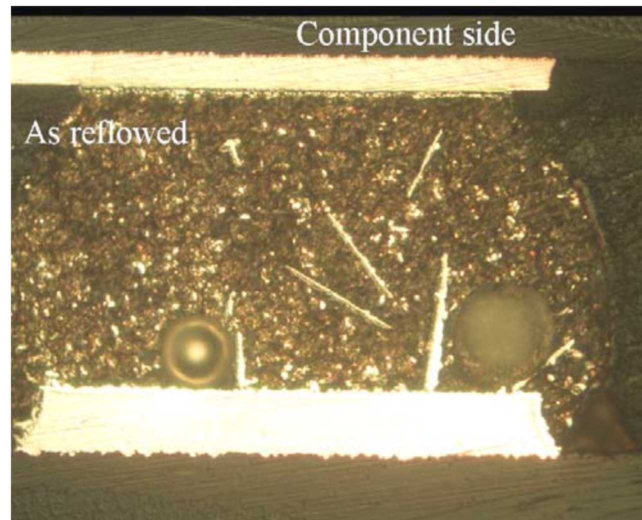


Figure 15: Needle like features in the microstructure of Sn3.0Ag0.5Cu solder (As-reflowed joint)

Figure 16 shows the magnified view of one of the needles shown in Figure 14. Point analysis function in the ESEM was utilized to analyze the elements at a specific point inside the needle. The electron beam size of 3 μm was selected such that the elemental spectrum is collected within the needle

Table 4 shows the results of the elements found and their composition at the analysis point. Also shown in the table is the expected composition of elements that form the Ag3Sn IMC from the SnAgCu phase diagram. From the SnAgCu phase diagram, the three elements Sn, Ag and Cu are expected to form three phases at room temperature, the Sn phase, Cu6Sn5 phase and Ag3Sn phase. Further data analysis was conducted to analyze the amount of each phase present by finding the percentage of each phase that can exist based on the elemental composition found. Results indicated 84% Ag3Sn, 7% Cu6Sn5 and 9% Sn phase, which verifies the composition of the needle to be rich in Ag3Sn phase.

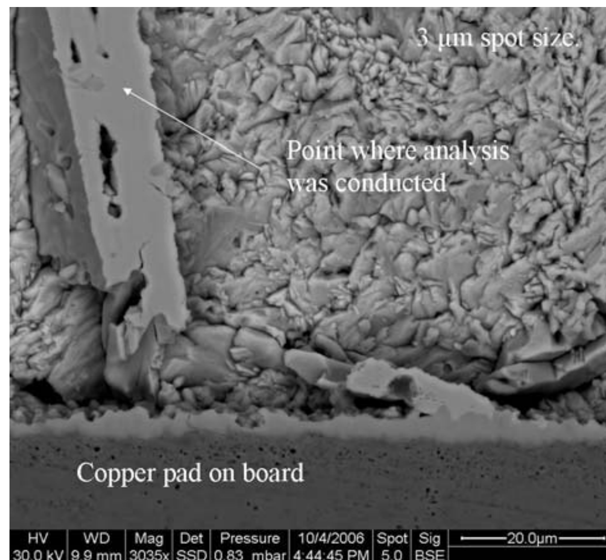


Figure 16: Magnified view of EDX analysis area from Figure 14

Table 4: Results of composition analysis conducted on a point from Figure 16

| Element | Measured Wt. % (S.D.) | Expected wt. % for Ag3Sn IMC from SnAgCu phase diagram [34] |
|---|---|---|
| Sn | 35.96 (0.53) | 26.83 |
| Ag | 61.60 (0.54) | 73.17 |
| Cu | 2.44 (0.21) | 0 |

Further etching of the tin, as depicted in Figure 17, revealed the three dimensional aspects of the Ag3Sn structures. Figure 18 shows the presence of these IMC in groups at the edges of the solder ball.

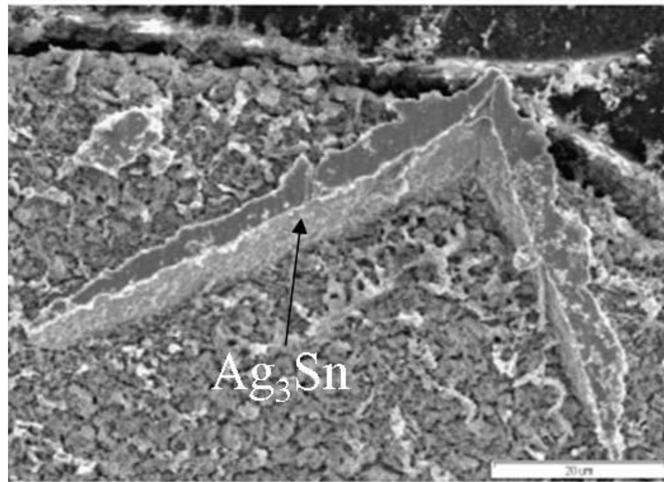


Figure 17: Solder joint of BGA component with Sn3.0Ag0.5Cu solder attached with Sn3.0Ag0.5Cu solder on board pad with ENIG finish showing Ag3Sn IMC – As-reflowed

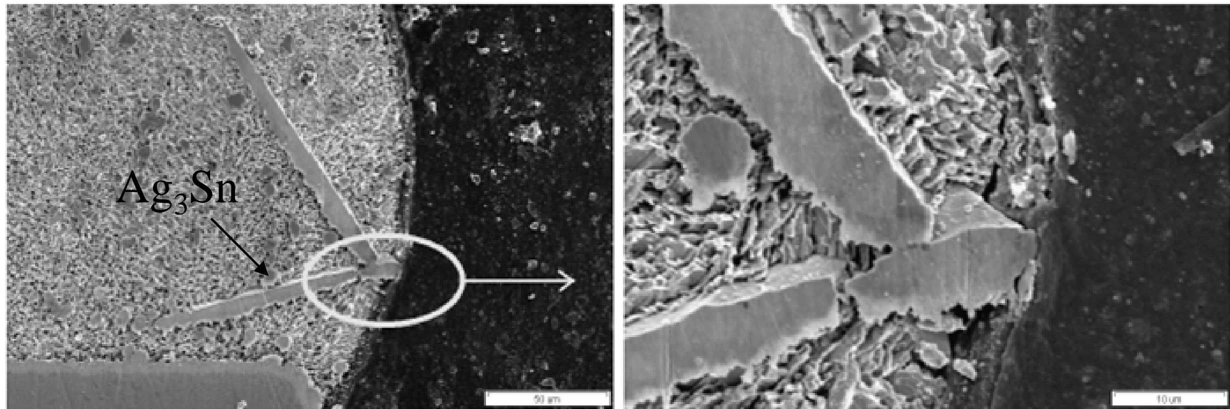


Figure 18: Solder joint of BGA component with Sn3.0Ag0.5Cu solder attached with Sn3.0Ag0.5Cu solder on board pad with OSP finish showing Ag3Sn IMC – Aged for 1000 hrs at 125ºC

To investigate the changes in the morphology of interfacial intermetallics under isothermal aging, component side intermetallics between solder and copper pad were analyzed. It was observed that for the as-reflowed joints the intermetallics layer is needle like (see Figure 19) and changes to a planar type after aging for 350 hours at 125ºC (see Figure 20).

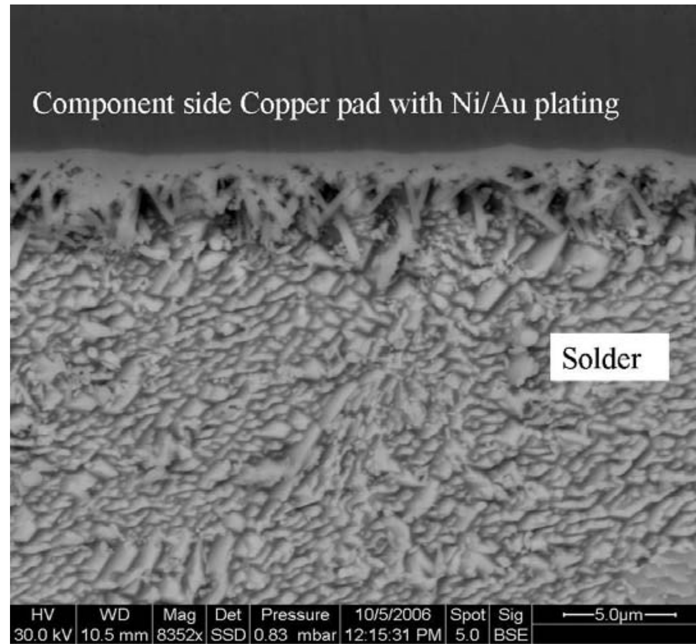


Figure 19: Needle type intermetallic layer for the as-reflowed joints

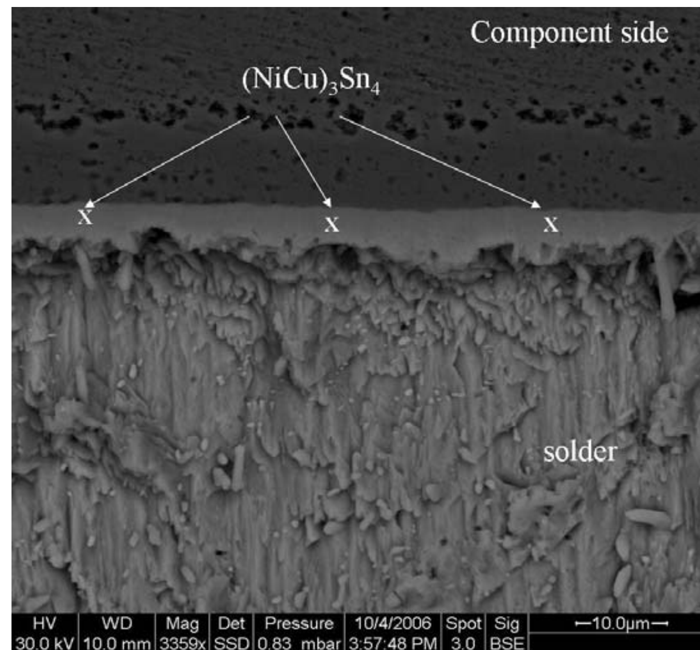


Figure 20: Planar intermetallics for the aged (125C for 350 hours) joints

### 3.5. "So-called" Kirkendal Voids

Microstructural analysis revealed the presence of microvoids at the interface between the solder and copper pad on the pcb. Microvoids at the interface between solder

and pcb pad are categorized into two major categories; champain voids those which are formed between bulk solder and IMC layer and kirkendal voids those formed between IMC and copper pad on pcb. Microvoids have been previously reported to be caused by the unbalanced interdiffusion of Cu and Sn at the interface between Cu pad and bulk solder, migration of Cu atoms leave vacancies on the Cu pad side and these vacancies are not filled by Sn atoms due to dissimilar diffusion rates, these vacancies coalesce and form microvoids [35]. Though microvoids have been previously reported [35][36] but the effect of microvoids on the reliability of solder joints is not well understood.

Figure 21, Figure 22 and Figure 23 show the as-reflowed, 350 hours aged and 1000 hours aged solder joints for ImSn finish respectively. It was observed that at the interface between IMC and copper pad, microvoids occur after 350 hours of aging and tend to increase in number with subsequent aging. Microvoids were found in ImSn, and HASL (SnPb) finishes for the solder joints aged at 350 and 1000 hours. Figure 24 shows the microvoids in the SnPb assembly after 350 hours of aging. For ImAg pad finish the location of voids were found to be between IMC and bulk solder (see Figure 25) instead of between IMC and copper pad as observed on other pad finishes.

Figure 21: Pad interface for ImSn finish (As-reflowed) with Sn3.0Ag0.5Cu solder joint

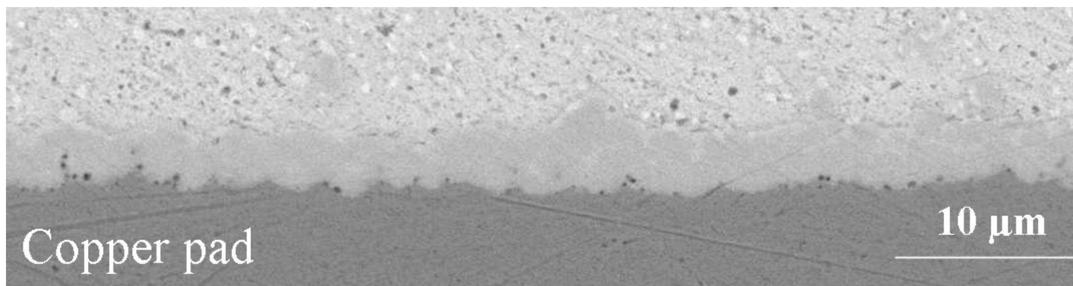


Figure 22: Pad interface for ImSn finish (Aged 125°C for 350 hrs) with Sn3.0Ag0.5Cu solder joint

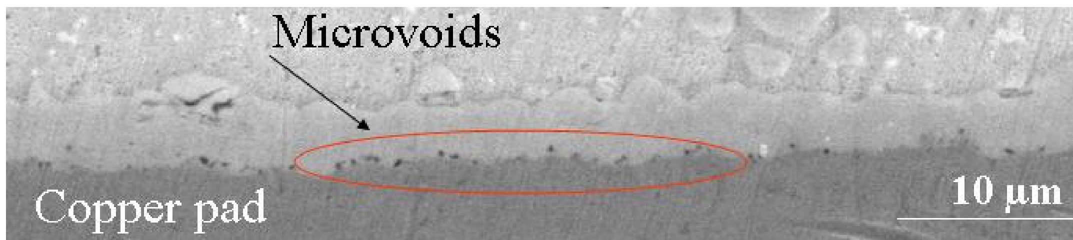


Figure 23: Pad interface for ImSn finish (Aged 125°C for 1000 hrs) with Sn3.0Ag0.5Cu solder joint

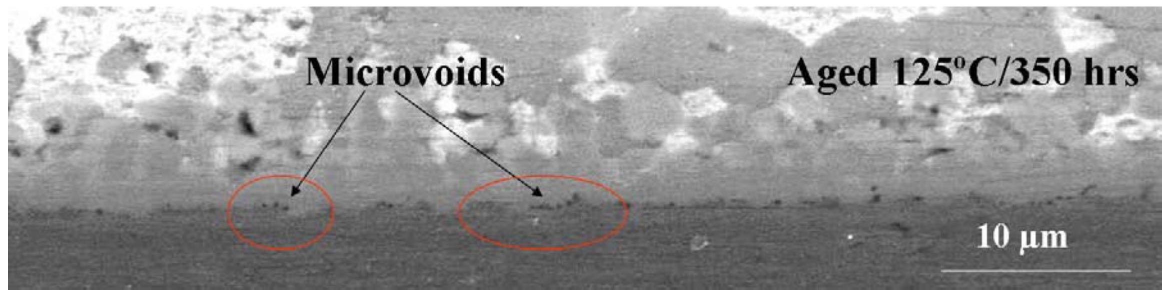


Figure 24: Pad interface for HASL finish (Aged 125°C for 350 hrs) with SnPb solder joint

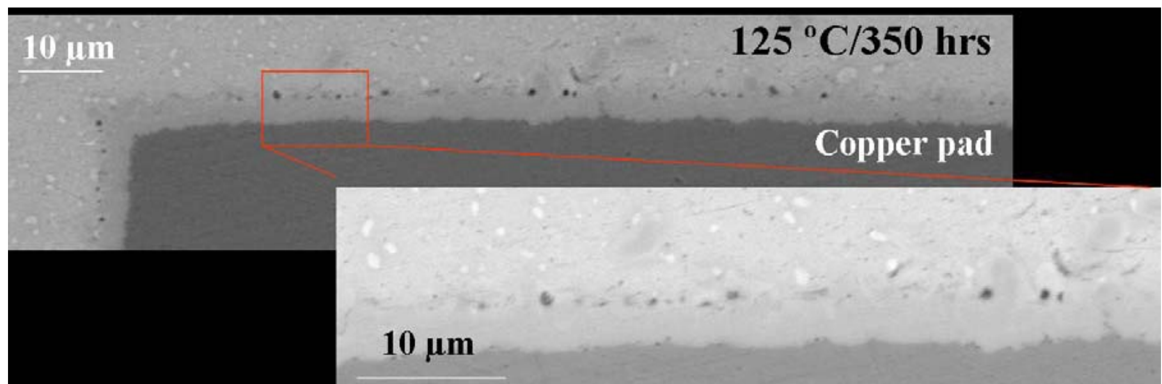


Figure 25: Pad interface ImAg pad finish - Sn3.0Ag0.5Cu solder joint (Aged 125°C for 350 hours)

Sections of the solder joints formed on ENIG pad finish showed appearance of blackpad. Blackpad has been reported to have an appearance of 'mud crack' at the interface between solder and Ni plating on copper [37]. Figure 26 shows the solder to copper interface for polyimide boards with ENIG pad finish and Figure 27 shows the magnified view of the interface showing appearance of delamination or crack.

Blackpad has been reported to cause brittle interfacial fracture of solder joints due to the segregation of phosphorus rich layer at the interface between Nickel and solder. The source of phosphorus comes from the electroless Nickel (Ni) plating method, where Ni is deposited as a mixture of Ni and Nickel-Phosphorus (Ni-P). More recent finding on

blackpad indicate that an aggressive attack of the electroless Ni plating during the immersion Au plating process may be causing the brittle fractures [38]. Elemental analysis was conducted using the EDX (Energy Dispersive X-ray) and the layer between solder and copper above the Ni layer was found to be phosphorus rich which indicated the possibility of the presence of blackpad.

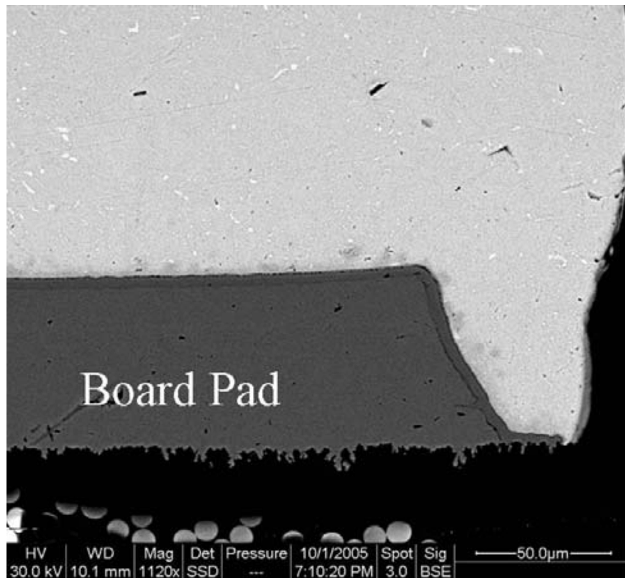


Figure 26: Black pad at the pad interface for ENIG- As-reflowed – Sn3.0Ag0.5Cu solder joint

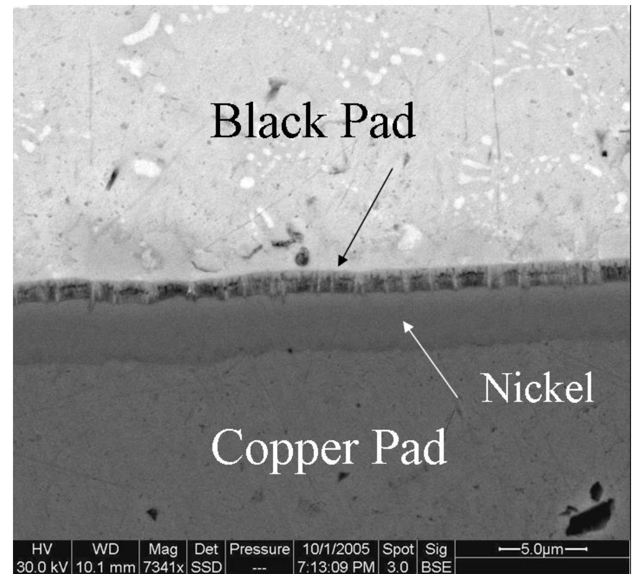


Figure 27: Black pad at the pad interface for ENIG-As-reflowed - Sn3.0Ag0.5Cu solder joint (Magnified view of pad interface)

### 3.6. Conclusions

This study was conducted to assess the effects of isothermal aging on composition and thickness of interfacial intermetallics formed with various pad finishes. Results indicated that after 350 hours of aging at 125°C, the IMC growth in solder joints with ImSn and ImAg are comparable whereas ENIG pad finishes show a lower IMC thickness

compared to ImSn and ImAg.  Lower IMC thickness for ENIG pad finish is due a low reaction rate of nickel with tin at high temperatures.

The thickness ranged from 2.5 to 3.5 μm after 350 hours of aging at 125°C. This growth is equivalent to the level anticipated after 10 years at 70°C based on the activation energy values of 1.03 eV for ImAg pad finish. Activation energy for ENIG and ImSn were found to be 0.54 ± 0.1 eV and 0.91 ± 0.12 eV. Activation energies for Sn-Ag-Cu based solders have been previously reported to be between 0.25 eV to 1.05eV and for SnPb to be 0.94 eV [31]-[33]. For Sn3.5Ag solder, the IMC thickness was affected by the pad finish. The thickness ranged from 1.5 to 4.5 μm after 350 hrs of aging and from 2.2 to 4.5 μm after 1000 hrs of aging.

For both Sn3.0Ag0.5Cu and Sn3.5Ag solders, ENIG pad finish resulted in thinner intermetallics. Due to less growth in IMC for ENIG finish compared to ImSn, ImAg and OSP, ENIG finish should be preferred for high reliability applications. On the other hand, ENIG finish is prone to black pad which forms during plating process. Solder joints should be investigated regularly to eliminate the possibility of black pad which can lead to early failures. Excess IMC would lead to early failures therefore finishes such as ImSn, ImAg and OSP should be avoided for high reliability application. As OSP is the cheapest finish compared to ImSn and ImAg and results in comparable IMC thickness, OSP finish could be used for short term reliability applications such as hand held devices and commercial electronics.

Champain void were found between the bulk solder and IMC in ImAg assemblies whereas kirkendal void were found between the IMC and copper substrate on ImSn and

SnPb control samples. Microvoids form after 350 hours of aging at 125ºC and the microvoids tend to increase in number with subsequent aging. Kirkendal voids are caused by the unbalanced interdiffusion of Cu and Sn at the interface between Cu pad and bulk solder. Migration of Cu atoms leave vacancies on the Cu pad side and these vacancies not filled by Sn atoms coalesce and form microvoids. ImAg finish has been known to be sensitive to plating chemistry and hence is prone to champain voids. Incoming assemblies should be inspected on a lot by lot basis to eliminate the possibility of microvoids those can lead to early failures.

# Chapter 4: MICROSTRUCTURE OF MIXED SOLDER JOINTS

## 4.1. Theory

Several studies[11][12][14][16][23], have been conducted to investigate the reliability of mixed solder joints subjected to various loading conditions and metallurgical combinations. For Pb-free BGA components assembled with Pb-based solder, the reliability has been shown to be equivalent to completely Pb-free assemblies, provided the Pb is distributed evenly throughout the joint. However, significantly earlier failures can occur if the Pb is not distributed in the mixed solder joint. From a manufacturing perspective mixed solder assemblies have a narrow window for the reflow temperature because of different melting temperatures of SnPb and Pb-free solders and the changes in solder volume depending on application. Due to the sensitivity to the mixing of Pb in the solder joints, process development should be conducted to develop a reflow process which would result in a homogeneous distribution of Pb over the entire solder ball. From a microstructural perspective, studies [17]-[22]have reported that a percentage of Pb greater than 3 % in a Pb-free solder will reduce the solidification temperature of Pb-free solder from 217ºC to 176 ºC. However, the significance of this solidification behavior on reliability has not been established.

Several studies have already focused on the effect of reflow on the microstructure of mixed solder joint [11][12][13] [18]. A fundamental understanding on the changes in microstructure is missing in the literature. This study is an effort to study the microstructural changes in mixed solder joints and determine the degradation mechanism in mixed solder joints. This study assesses the reliability of mixed solders as a function of

the microstructural changes that can occur during environmental storage and operation. This study focuses on the microstructural characterization for mixed solder joints. Two microstructural features namely, Pb phase coarsening and intermetallic compounds were analyzed for mixed solder microstructure under various isothermal aging conditions. A Pb phase study was conducted to evaluate the extent of coarsening in the bulk of mixed solder as compared to SnPb. An intermetallic study was then conducted to analyze the growth and composition of IMC for mixed solder joints.

### 4.2. Experimental design

In our studies, BGA components were assembled onto circuit boards, at a high volume assembly house, using Sn37Pb and Sn3.0Ag0.5Cu solders, and various board pad finishes: immersion tin (ImSn), immersion silver (ImAg), electroless nickel-immersion gold (ENIG) and hot air solder leveled (HASL). The assembly matrix is shown in Table 5. Board assemblies were aged at 125 ºC for durations of 100, 350, and 1000 hours after the reflow process. Control assemblies (no ageing) were also included for each assembly combination. To simulate a typical solder joint in an industrial surface mount process, assemblies for this test were prepared in a qualified high volume contract manufacturing house having a developed and qualified SnPb, Pb-free and mixed reflow assembly process.

**Table 5: Circuit board solder and pad finish assembly matrix**

| Identifier | BGA Solder ball | Solder paste | Reflow condition | Pad finish |
|---|---|---|---|---|
| Mixed | Sn3.0Ag0.5Cu | Sn37Pb | Peak temperature: 220°C, time above liquidus: 67-70 sec, cooling rate: 2°C/sec | ImSn, ImAg, ENIG, HASL (SnPb) |
| Pb-free | Sn3.0Ag0.5Cu | Sn3.0Ag0.5Cu | Peak temperature: 245°C, time above liquidus: 77-81 sec, cooling rate: 2.1°C/sec | ImSn, ImAg, ENIG |
| SnPb | Sn37Pb | Sn37Pb | Peak temperature: 215°C, time above liquidus: 67-70 sec, cooling rate: 1.8°C/sec | HASL (SnPb) |

### 4.3. Lead (Pb) phase distribution and coarsening

To determine the distribution of Pb in the microstructure, first the behavior of Pb during solidification was analyzed. The maximum solubility of Pb in Sn, is observed to be 3.4% from the SnPb phase diagram. When the volume of Pb is greater than 3.4%, residual Pb will precipitate in Sn grain boundaries. The diffusion of Pb in solder at 200°C (below Pb-free melting temperature 217°C) was calculated from Equation 1[44]:

$$D = 5.1\exp(\frac{-41000}{RT}) = 1.5 \times 10^{-4}\ \text{cm}^2/\text{sec} \qquad \text{Equation (1)}$$

$$t = \frac{L^2}{D} \qquad \text{Equation (2)}$$

The diffusion time (t) is found to be 6 sec, where D is the diffusivity for Pb in Sn [44], R is 8.314 (J)(K-1)(mol-1), T is temperature in K, and L is the characteristic length of diffusion ~300 μm (solder joint height). Since the diffusion coefficients of solute atoms in liquid are much larger than in solids, the diffusion relation for solid (equation 1) can be considered in calculating the diffusion length for Pb in solder for reflow during time above liquidus. Length of diffusion (L) during the time above liquidus (t) of 60 sec (typical time above liquidus) can be calculated by equation 2, which gives a characteristic length of 900 μm. Since the height of solder joint is ~ 300 μm, Pb will diffuse through out the solder during reflow.

To understand the location of Pb in the solder a quaternary phase diagram was considered [18]. Phase diagram suggests that the melting temperature of solder decreases from 217ºC to 176 ºC due to the presence of Pb and the last liquid to solidify contains Pb. This can also be confirmed from ternary phase diagrams of Sn-Cu-Pb which suggests that the last liquid to solidify contains Pb (see Table 6).

**Table 6: Composition of phase at last solidification temperature (181°C) for Sn-Cu-Pb system**

| Reaction | Phase | Mass % Cu | Mass % Pb | Mass % Sn |
|---|---|---|---|---|
| L → (Sn) + (Pb) + $Cu_6Sn_5$ [26] | Liquid | 0.09 | 37.27 | 62.64 |
| | $Cu_6Sn_5$ | 39.07 | 0 | 60.93 |
| | (Pb) | 0 | 81.23 | 18.77 |
| | (Sn) | 0 | 3.39 | 96.61 |

In this study, the amount of coarsening in mixed solder joints was compared to SnPb solder joints. Phase coarsening is generally referred to as Ostwald ripening. A reduction in the total interfacial energy provides the driving force for coarsening. The

process results in an increase in the distance of separation between neighboring particles and in a decrease in the number of particles in the system. The thermodynamic basis of coarsening in alloys is the Thompson-Freundlich solubility relationship, according to which, the Pb concentration in a Sn-rich matrix adjacent to a Pb-rich particle is in proportion to its radius of curvature when the phases are in local equilibrium. Upon exposure to thermal aging, Pb-rich particles dissolve in Sn-rich matrix causing an increase in Pb concentration adjacent to the Pb-rich particle. As atoms diffuse from a region of higher concentration to lower, Pb atoms will diffuse from small particle to the larger particle to make up for the reduction in concentration near the larger Pb-rich particle. Diffusion of Pb atoms away from the smaller Pb-rich particle causes a reduction in its radius of curvature.

As the flow of atoms proceeds, small particles dissolve to compensate for the decrease in concentration at their interface. Larger distance between the Pb-rich particles will require longer time for the diffusion process thus influencing the amount of coarsening that is observed after 350 hrs at 125ºC. In mixed solder joints, due to the larger average distance between Pb-rich particles, an equivalent amount of coarsening would require time longer than 350 hrs as compared to SnPb solder joint. Thus in mixed solder joints no significant coarsening is visible after 350 hrs of aging at 125ºC.

IMAGEPRO 4.5.1 commercial image analysis software was utilized to quantify the Pb phase in the microstructure before and after aging. Pb phases were considered as spherical shape and the diameters of the particles where plotted with respect to aging condition. Analysis was conducted over the entire solder ball and the total area of Pb in the solder joint was plotted in bars (see Figure 28). For this analysis, 16 balls were

analyzed per BGA component and were found to be optimal number to get a statistical confidence. The Pb phase region was found to reduce with aging (350 hours at 125 °C) for mixed solder joint (see Figure 29 and Figure 30), whereas it increased for SnPb solder joints (see Figure 31 and Figure 32). The lack of coarsening in mixed solder can be attributed to an insufficient concentration gradient between Pb phases due to a larger separation distance between Pb phases in mixed solder joints (see Figure 33) compared to SnPb joints (see Figure 34). However, a higher quantity of Pb and a smaller separation distance between Pb phases in SnPb solder produces a sufficient concentration gradient to promote the coarsening process.

**Figure 28: Comparison of change in Pb phase area for mixed and SnPb solder joints due to aging.**

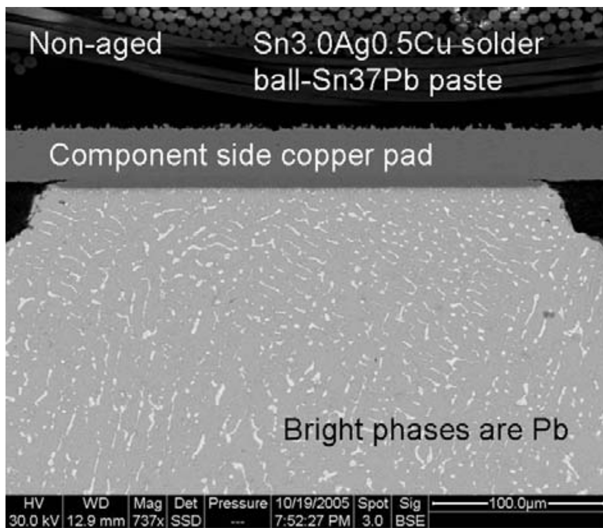


Figure 29: Distribution of Pb phase in mixed solder joint (non aged)

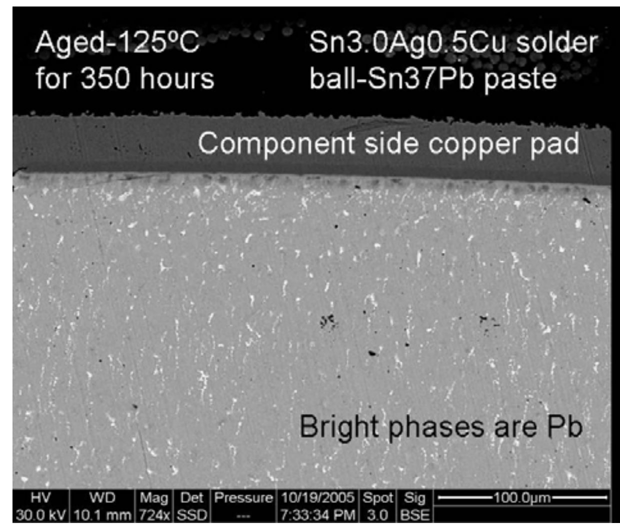


Figure 30:Distribution of Pb phase in mixed solder joint aged (350 hours at 125 ºC)

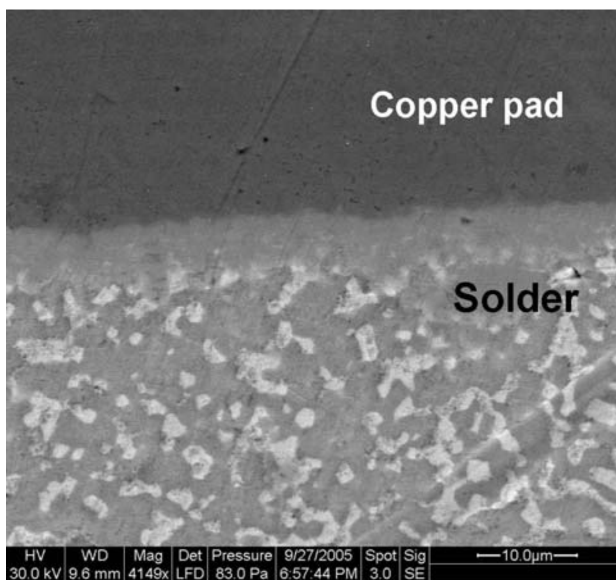


Figure 31: Distribution of Pb phase in SnPb solder joint (Non aged)

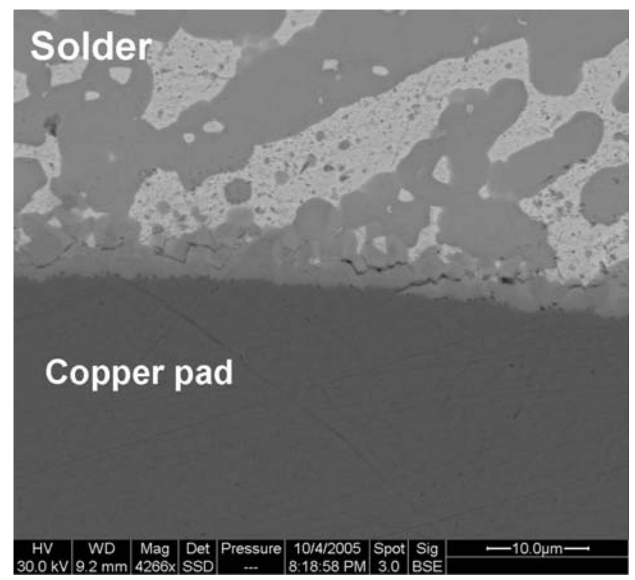


Figure 32: Distribution of Pb phase in SnPb solder joint aged (350 hours at 125 ºC)

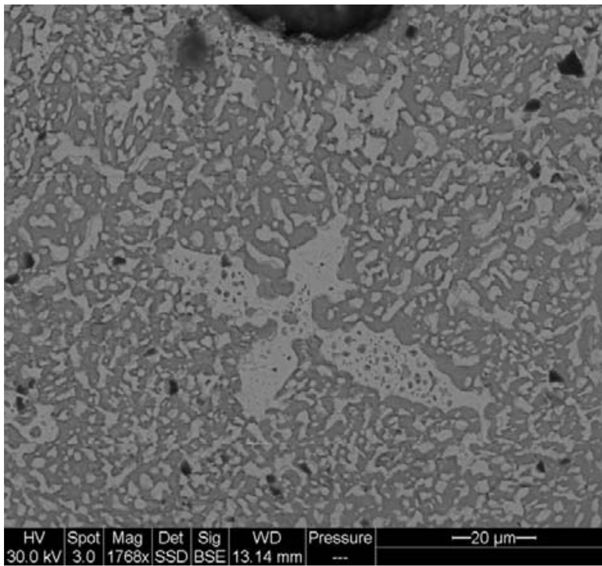


**Figure 33: SnPb solder joint – As reflowed**

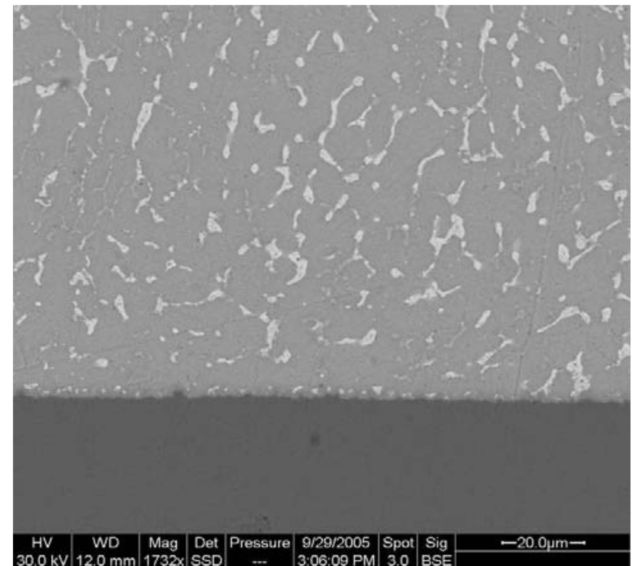


**Figure 34: Mixed (SnAgCu BGA assembled with SnPb paste) solder joint - As reflowed**

### 4.4. Intermetallic compound thickness analysis

The solder joint assembly process involves the interaction of metallurgies from the component, board, and solder. Intermetallic compounds (IMC) are formed due to the inter-diffusion of dissimilar materials, governed by thermally activated diffusion process. The initial formation of IMCs during soldering ensures a good metallurgical bond. However, the growth of these IMCs results in a brittle interface that leads to failure under high stress loading, such as shock and vibration [50].

To investigate IMCs, samples were polished and then etched to enhance the contrast of elements under scanning electron microscope (SEM). Etching was conducted using a solution of 2 % HCL (30 % conc.), 5 % $HNO_3$ (70 % conc.), and ethanol. A five second etching time was used for each sample. IMC composition was analyzed both at the component side and board side for the BGA component. Pictures of solder joint

cross-sections were taken using an optical microscope with polarized light to clearly demarcate the IMC layer. IMC thickness measurements taken on optical images were verified using SEM. Three solder joints per sample were analyzed and three measurements per solder joint were taken.

Figure 35 shows the IMC thickness for various pad finishes for Sn3.0Ag0.5Cu and Sn37Pb solder. After 350 hours of aging at 125 °C, an IMC thickness range of 2.5 to 3.5 µm was observed for all pad finishes. After 1000 hours of aging at 125 °C, the IMC thickness was approximately 3 to 3.5 µm for ImAg and ImSn, whereas 2.8 µm for ENIG. The lower IMC thickness in ENIG pad finish is due to the presence of nickel layer on copper pad which acts as a barrier layer for diffusion of copper and tin restricting the formation of IMC. Comparing the IMC thickness for SnPb and Pb-free solder joints with that of mixed solder joints, it was found that IMC thickness for mixed solder joints was 30 to 40% lower (see Figure 36).

The lower growth of IMCs in the case of mixed solder joints can be attributed to the segregation of Pb at the interface of solder and copper pad (see Figure 37 and Figure 38). The presence of Pb retards the formation of IMCs by influencing the diffusion of Sn and Cu at the interface. As it can be observed from SnPbCu phase diagram that, any dissolution of Cu into the solid solder brings the solder into the Sn+Pb+$Cu_6Sn_5$ three phase field. At the interface, Cu reacts with Sn to form $Cu_6Sn_5$ IMC by consuming the Sn from the solder. Due to the slower diffusivity of Pb in the solid solder (diffusivity of Pb in solder is about $10^{-8}$ $cm^2$/sec and for Cu is $10^{-6}$ $cm^2$/sec), the depletion of Sn in the solder can lead to higher concentration of Pb in the solder next to $Cu_6Sn_5$. This phenomenon leads to the deposition of a thin layer of Pb between the solder and the

$Cu_6Sn_5$ IMC layer [49]. Due to the deposition of Pb, the diffusion of Sn and Cu is restricted. Segregation of Pb on the component side was also observed in this study, with the presence of Ni. Pb segregation at the interface with the presence of Ni in the pad finish has been previous reported [63] for SnPb solders. Deposition of Pb, due to aging in mixed solder joint, would restrict IMC formation, whereas in Pb-free solders IMC can form without any restriction of Pb.

Composition of IMC for Pb-free and mixed solder joints were determined using energy dispersive X-ray (EDX) facility in SEM. On the board side, for mixed solder joints the IMC layer was composed of $Cu_6Sn_5$ and $Ag_3Sn$ IMC (see Figure 39 and Figure 40). A list of IMCs found at the interface is listed in Table 7.

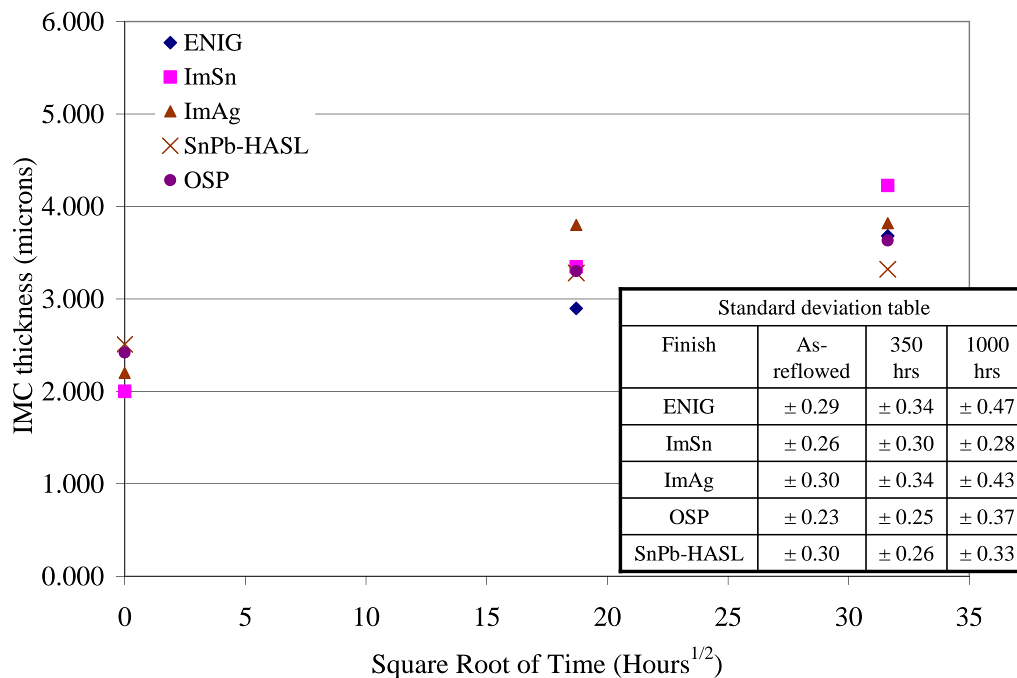


Standard deviation table

| Finish | As-reflowed | 350 hrs | 1000 hrs |
|---|---|---|---|
| ENIG | ± 0.29 | ± 0.34 | ± 0.47 |
| ImSn | ± 0.26 | ± 0.30 | ± 0.28 |
| ImAg | ± 0.30 | ± 0.34 | ± 0.43 |
| OSP | ± 0.23 | ± 0.25 | ± 0.37 |
| SnPb-HASL | ± 0.30 | ± 0.26 | ± 0.33 |

**Figure 35: Intermetallic growth for Pb-free and SnPb solder joints due to aging at 125 °C.**

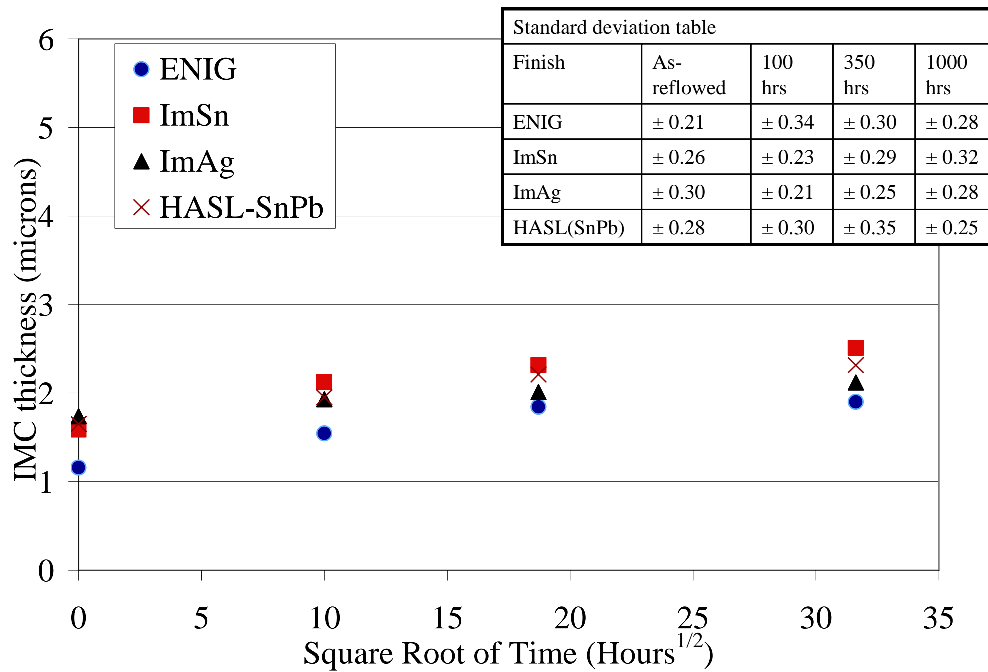

| Standard deviation table | | | | |
|---|---|---|---|---|
| Finish | As-reflowed | 100 hrs | 350 hrs | 1000 hrs |
| ENIG | ± 0.21 | ± 0.34 | ± 0.30 | ± 0.28 |
| ImSn | ± 0.26 | ± 0.23 | ± 0.29 | ± 0.32 |
| ImAg | ± 0.30 | ± 0.21 | ± 0.25 | ± 0.28 |
| HASL(SnPb) | ± 0.28 | ± 0.30 | ± 0.35 | ± 0.25 |



**Figure 36: Intermetallic growth for mixed solder joints (Sn3.0Ag0.5Cu solder balls attached with Sn37Pb solder) due to aging at 125 °C.**

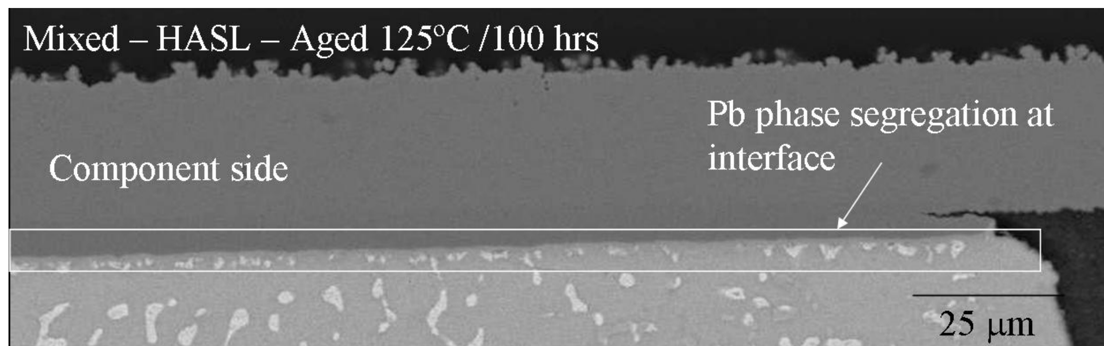


**Figure 37: Segregation of Pb at the component side for mixed solder joint (Pb-free solder balls-SnPb solder paste)**

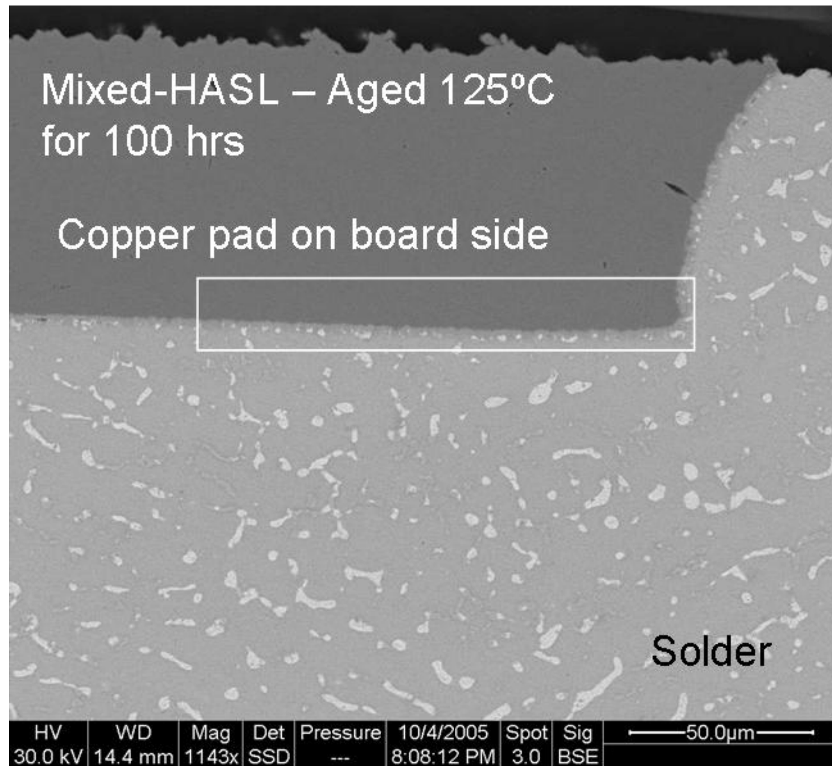


**Figure 38: Segregation of Pb at the board side for mixed solder joint (Pb-free solder balls-SnPb solder paste)**

**Table 7: Type of IMCs for Several Pad Finishes**

| Finish | Type of IMC |
|---|---|
| ENIG | $(Cu,Ni)_6Sn_5$, $(Ni,Cu)_3Sn_5$, $(Au,Ni)Sn_4$ |
| ImSn | $Cu_6Sn_5$, $Cu_3Sn$ |
| ImAg | $Cu_6Sn_5$, $Cu_3Sn$, $Ag_3Sn$ |
| OSP | $Cu_6Sn_5$, $Cu_3Sn$ |

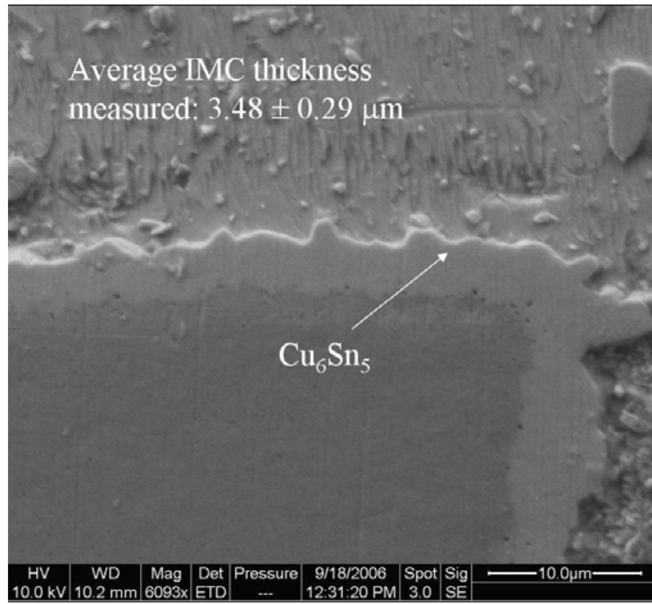


**Figure 39: Sn3.0Ag0.5Cu solder joint on ImSn pad finish (aged at 125 °C for 350 hrs) showing IMC thickness.**

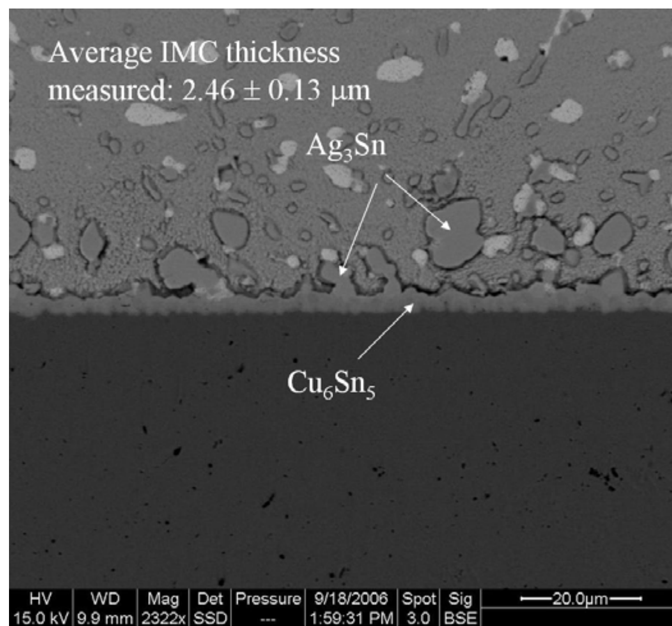


**Figure 40: Mixed solder joint on ImSn pad finish (aged at 125 °C for 350 hrs) showing lower IMC thickness than Pb-free joint.**

### 4.5. Discussion and Summary

The global transition to Pb-free electronics has raised concerns among manufacturers with mixing of SnPb and Pb-free metallurgies. Along with loading conditions, microstructure plays a key role in the reliability of solder joints. This study examines two aspects related to mixed solder joint microstructure; Pb phase coarsening in bulk solder and IMC formed at the interface of solder-copper pad finish.

Isothermal aging indicated negligible coarsening of Pb in the mixed solder joints. The lack of coarsening in mixed solder is attributed to an insufficient concentration gradient due to a larger separation distance between Pb phases compared to SnPb solder joint. It is partly this absence of coarsening of the Pb phase which results in mixed solder joints having a better fatigue resistance in thermal cycling compared to SnPb solder joints.

Interfacial intermetallics indicate that mixed solder joints result in 30 to 40% lower IMC thickness than SnPb and Pb-free. Lower IMC thickness in mixed solder joint is attributed to the presence of a Pb-rich layer found at the interface between solder and copper pad, which in turn tends to retard the growth of intermetallics in mixed solder joints. The presence of Pb-rich interface acts as a diffusion barrier between the base metal copper and solder. With less IMC formation at the interface, the mixed solders should have better fatigue resistant compared to completely SnPb or Pb-free joints.

Thermal cycling fatigue failures occur in the region of high stress concentration in the bulk solder. Presence of Pb in the solder causes reduction in solder joint reliability due to coarsening under thermal cycling [6][7]. Due to the coarsening behavior of Pb,

SnPb solder joints are less durable than Pb-free solder joints subject to thermal fatigue loading. Mixed solder joints are more resistant to coarsening phenomena and hence result in joints with better thermal fatigue resistance compared to eutectic SnPb joints. Thermal fatigue performance of mixed solder joints have been reported to be comparable to SnAgCu for BGA components [11][14][16]. Which supports the finding in this paper that mixed solder joints will have comparable thermal fatigue performance compared to Pb-free solder joints and better than SnPb due to the insignificant coarsening behavior.

Failures in high loading environments such as vibration and shock, occur at interfacial intermetallic layers. Studies [50] have reported that under drop test, failures occur in IMC layer and drop reliability decreases with increase in IMC thickness. This study suggests that because the thickness of intermetallics layer for mixed solder joints is smaller than with SnPb and Pb-free; they are expected to perform better under vibration and shock conditions.

For Pb-free BGA components assembled with Pb-based solder, the reliability has been reported to be equivalent to completely Pb-free assemblies, provided the Pb is distributed evenly throughout the solder joint. However, significantly earlier failures can occur if the Pb is not distributed. From a microstructural perspective, changes occurring in mixed solder joints exhibit different characteristics than conventional SnPb and Pb-free solder joints which must be accounted for when predicting the reliability of solder joints.

# Chapter 5: RELIABILITY TEST

## 5.1. Theory

For several years, the reliability of lead-free solder interconnects has been the subject of intense investigation. Under temperature cycling loading, lead-free solder interconnects have generally been demonstrated to be as good as or better than tin-lead solder interconnects. Exceptions have been with non-compliant interconnects such as those formed with ceramic leadless chip carriers and leadless chip resistors subjected to extreme temperature cycles (e.g. -55 to 125C)[51]. However, under lower temperature ranges and for lower cyclic mean temperatures, lead-free assemblies show a significantly longer life as compared to tin-lead assemblies of similar construction [52].

In reviewing the literature, there appears to be little information on the impact of isothermal aging on lead-free solder interconnects reliability. Isothermal aging plays a significant role in the growth and composition of intermetallics within solder interconnects. Intermetallic compounds (IMC) are formed due to diffusion of two dissimilar materials, governed by a thermally activated diffusion process. Intermetallic compounds form within the bulk solder and at the interfaces between the bulk solder and metal contacts of printed circuit board (PCB). The initial formation of intermetallic compounds (IMC) during soldering ensures a good metallurgical bond. However, the growth and composition of IMCs can compromise reliability and have been associated with early failures [41][42].

Though microstructural changes of bulk solder intermetallics have been reported in several studies [53][54], their influence was not correlated with fatigue life. Anna et.

al., [55], investigated effect of isothermal aging on pull strength of BGA solder joints. It is stated in the study that solder joint failures occur due to brittle fracture along the brittle IMC layer present between the solder and pcb pad. Upon exposure to longer aging times and higher aging temperatures, IMCs increase in thickness and result in lower pull strengths. Pull test is a high stress test wherein the fracture occurs along the brittle IMC layer at the interfacial IMC. Whereas, for certain loading conditions such as thermal cycling, solder joint failures occur in a ductile manner along the region of high stress concentration in bulk solder and the IMC changes in the bulk solder under isothermal aging play a key role. Therefore as opposed to the interfacial IMC characterized which play a key role in high stress, this study focuses on IMC's in the bulk solder, which play a key role in thermal cycling failures. The most common lead-free solders are composed of elements such as tin (Sn), copper (Cu) and silver (Ag) which can form intermetallic compounds such as $Cu_6Sn_5$ and $Ag_3Sn$ in the bulk solder and can impact the reliability of lead-free solder joints.

This study investigates the impact of isothermal aging on the temperature cycle reliability of solder interconnects. In this assessment, lead-free and tin-lead assemblies of similar construction were isothermally aged and subjected to a temperature cycle tests. As a control, none aged assemblies were also tested. Microstructural analysis was performed on both aged and non-aged specimens and failure analysis was conducted on temperature cycled test specimens.

## 5.2. Design of Experiment

In this study, test assemblies of similar construction were created with Sn37Pb and lead-free (Sn3.0Ag0.5Cu) solders. The components under test were 256 IO, 1 mm pitch plastic ball grid arrays. The lead-free version of the PBGA had Sn3.0Ag0.5Cu solder balls, while the tin-lead version had Sn37Pb solder balls. The assembled solder joints were solder-mask-defined on the component side and pad-defined on the board side. The assembly matrix is shown in.

Table 8

The test boards were constructed of low-Tg FR4 board. The board metallization on the lead-free assemblies was immersion tin (ImSn), while the tin-lead assemblies used tin-lead hot air solder leveled (HASL) finish. Half to the test specimens were isothermally aged at 125ºC for 350 hours. Isothermal aging is expected to result in the growth of intermetallic interfaces between the bulk solder and the component and board pads, respectively. This stated aging condition has been equated to IMC formation after 10 years at 70ºC [8]. Non-aged board assemblies were included as control. Baseline isothermal aging conditions were chosen with respect to microstructural changes reported to occur at 125ºC for 350 hours [32][33].

**Table 8: Board assembly matrix**

| Identifier | BGA solder ball | Solder paste | Board pad finish | Aging condition | BGA components |
|---|---|---|---|---|---|
| Lead-free | Sn3.0Ag0.5Cu | Sn3.0Ag0.5Cu | ImSn | Non-aged | 8 |
| | | | | Aged (350 hours at 125°C) | 8 |
| Tin-lead | Sn37Pb | Sn37Pb | HASL tin-lead | Non-aged | 8 |
| | | | | Aged (350 hours at 125°C) | 8 |

After isothermal aging, the test specimens were subjected to temperature cycling between -40°C to 125°C with 15 minute dwells at temperature extremes. These accelerated testing conditions are recommended under JEDEC standard JESD22-A104C (Temperature Cycling) and have been used in several studies [32][42] to test for temperature cycle fatigue reliability of solder joints. In situ resistance monitoring was conducted to detect solder joint failure during temperature cycling. Failure was defined as one or more resistance excursions greater than 300 ohms occurring in ten consecutive temperature cycles, in conformance with IPC-SM-785 (Guidelines for Accelerated Reliability Testing of Surface Mount Solder Attachments).

### 5.3. Reliability test results

The time to failure data from the temperature cycle test was analyzed to compare the reliability of non-aged and aged solder joints. An acceptable correlation parameter ($\rho$) was achieved by using Weibull two parameter distribution. The data shows that the stated aging condition results in a twenty-five percent reduction in characteristic life ($\eta$) with 85% confidence for tin-silver-copper lead-free solder joints compared to the non-aged lead-free assemblies (see Figure 41). No significant change was observed for tin-lead solder joints with 95% confidence bounds (see Figure 42).

A wider distribution was observed for aged lead-free solder joints compared to non-aged lead-free joints. Isothermal aging results in formation of intermetallic compounds those may also play a role in the wider failure distribution measured for the aged lead-free specimens as compared to the non-aged lead-free specimens. These particles may also in part explain the general wider failure distribution observed with tin-silver-copper solder as compared with tin-lead solder interconnects. Further analysis was conducted to investigate the changes in the microstructure of lead-free solder joints after isothermal aging.

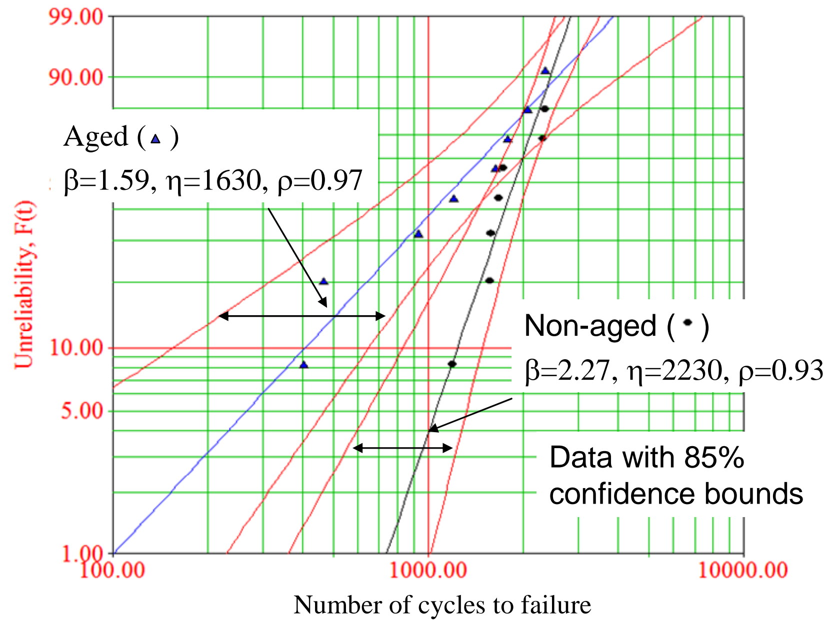


**Figure 41: Reliability results indicating 25% reduction in characteristic life (η) of aged compared to non-aged lead-free joints (β is the slope and ρ is the correlation coefficient)**

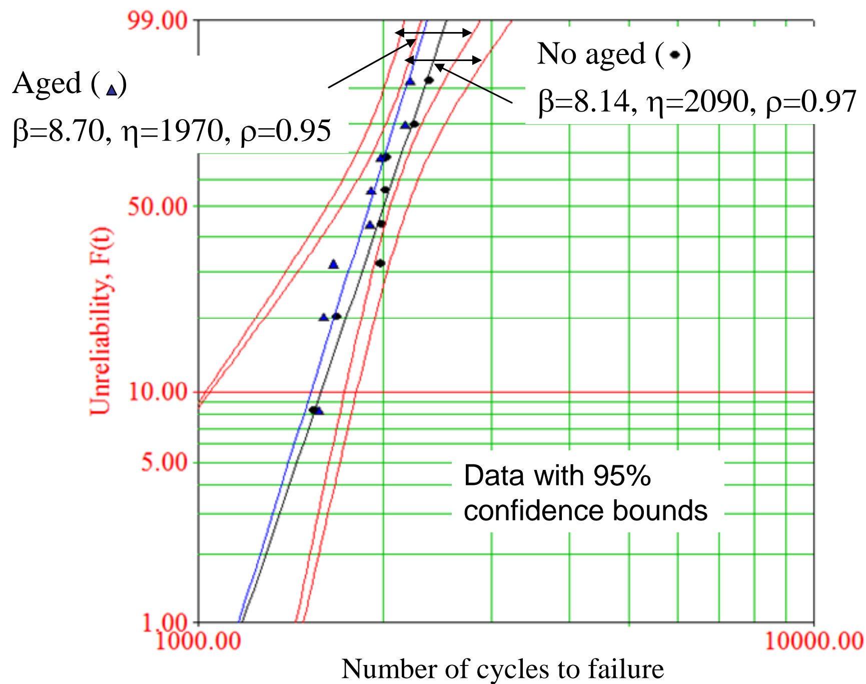


**Figure 42: Reliability comparison of aged and non-aged SnPb solders joints showed no significant difference in characteristic life**

### 5.4. Physical microscopic analysis

To assess the influence of isothermal aging on the temperature cycle fatigue life of solder interconnects, the microstructure of non-cycled non-aged and aged (350 hours at 125ºC) solder joints were examined. Sectioned solder joints were prepared by cutting individual BGAs from the printed wring board assembly, potting the extracted BGA in an epoxy compound, cutting the potted sample with a diamond saw, and using various grades of sandpaper prepare the samples. The samples were then polished and etched to enhance the contrast of microstructural features. Etching was conducted using a solution of 2 % HCL (30 % conc.), 5 % $HNO_3$ (70 % conc.), and ethanol. A five second etching time was used for each sample. After etching, solder joints were examined under an optical microscope with a polarized light. As tin is a birefringent material, different crystallographic orientations of tin grains exhibit distinguishable contrast under polarized light.

As shown in Figure 43, as-reflowed lead-free interconnects contain only several colonies, which are clusters of Sn grains. The Sn grains inside each colony are almost uniformly oriented and can not be distinguished easily, but the colonies can be clearly seen due to the large orientation difference at the boundaries. The large angle grain boundary is verified under scanning electron microscope (SEM) (see Figure 45). This is in accordance in the previous studies in literature [65].

Isothermal aging may introduce some changes to the colonized microstructure of solder joints. It is observed that the number of colonies decrease after isothermal aging. Out of the ten solder balls analyzed the number of colonies for non-aged joints ranged

between three to seven with an average of five (see Figure 43), whereas for aged joints colonies ranged from two to four with and average of three (see Figure 44). This might be a result of grain size growth. Since interfacial energy is relatively high at large angle boundaries, reducing number of colonies should be favored during isothermal aging.

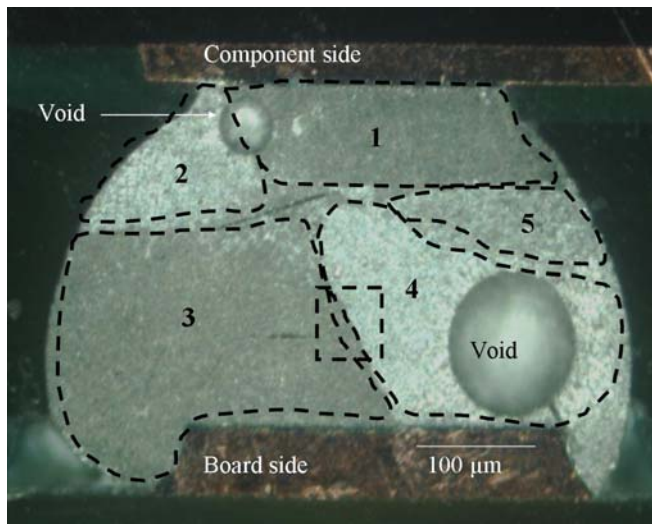


**Figure 43: Optical polarized image of as- reflowed Sn3.0Ag0.5Cu BGA joint showing tin grain colonies in the bulk solder (Grain colonies are marked by number 1 to 5)**

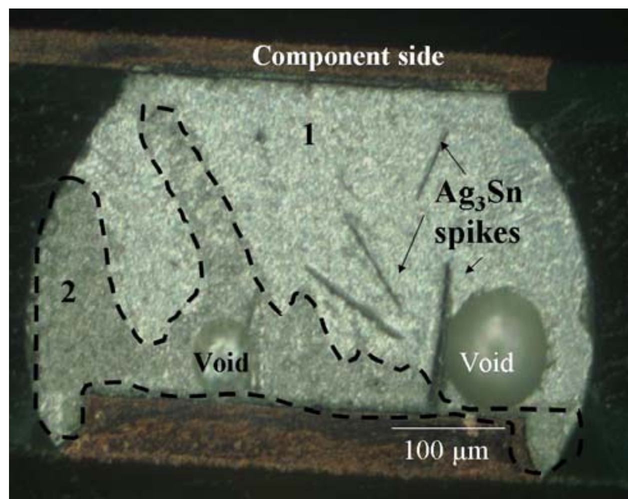


**Figure 44: Optical polarized image of Sn3.0Ag0.5Cu BGA joint aged at 125ºC for 350 hours showing tin grain colonies in the bulk solder (Grain colonies are marked by number 1 to 2)**

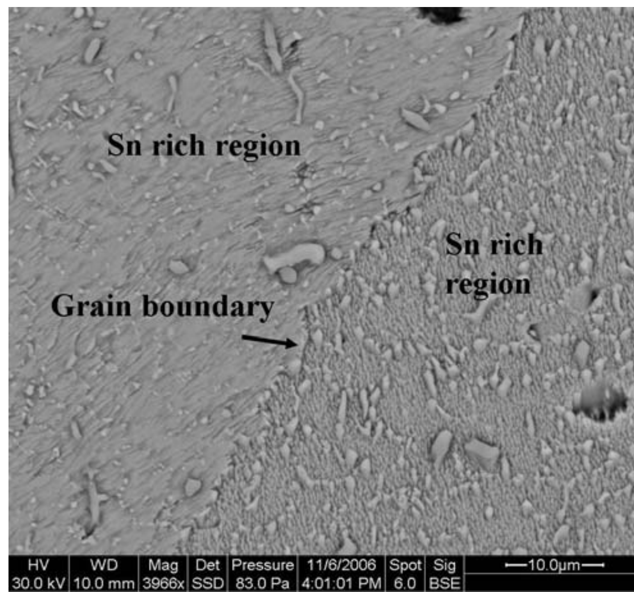


**Figure 45: SEM image showing grain colony boundary between tin grains 3 and 4 in Figure 43**

The presences of intermetallics within the tin-silver-copper lead-free solder may also influence temperature cycling fatigue life of solder interconnects. Figure 46 shows tin-copper and silver tin intermetallics distributed within a non-aged tin-silver-copper solder interconnect. To assess the intermetallics in the tin-silver-copper solder between non-aged and aged test specimens, the number intermetallic particles in the solder were measured. For this assessment, the etching time was increased to 10 seconds using the previously discussed solution. Number of IMC particles in the bulk solder was counted using image analysis software. An acceptable statistical confidence was achieved by evaluating nine solder balls for each non-aged and aged specimens. Figure 46 shows the IMC in the bulk solder for non-aged solder joints and Figure 47 for aged. It was observed that non-aged solder joints had a significantly greater amount of IMCs in the bulk solder as compared with aged solder joints (see Figure 48).

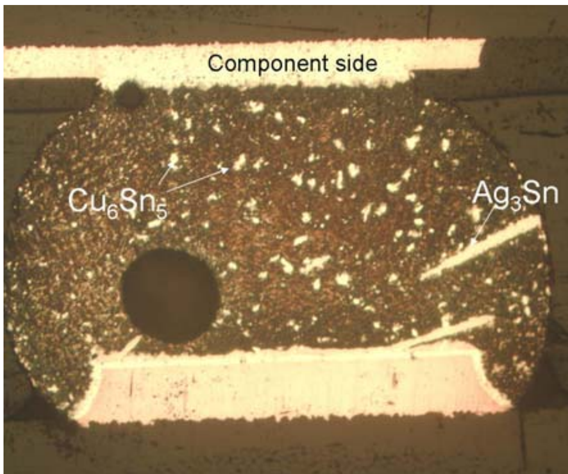


**Figure 46: Presence of IMC in bulk solder of non-aged lead-free solder joint (Etched solder joint)**

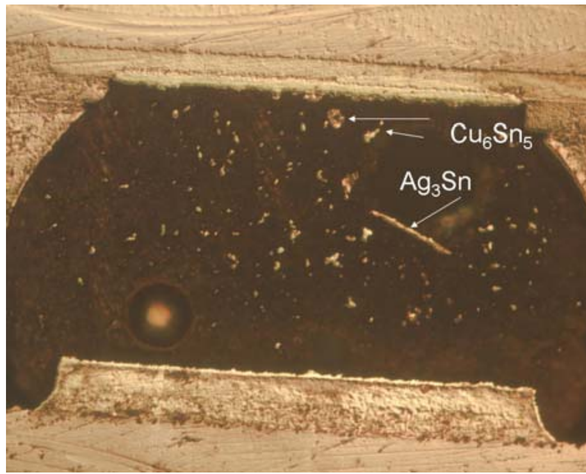


**Figure 47: Presence of IMC in bulk solder of aged lead-free solder joint (Etched solder joint)**

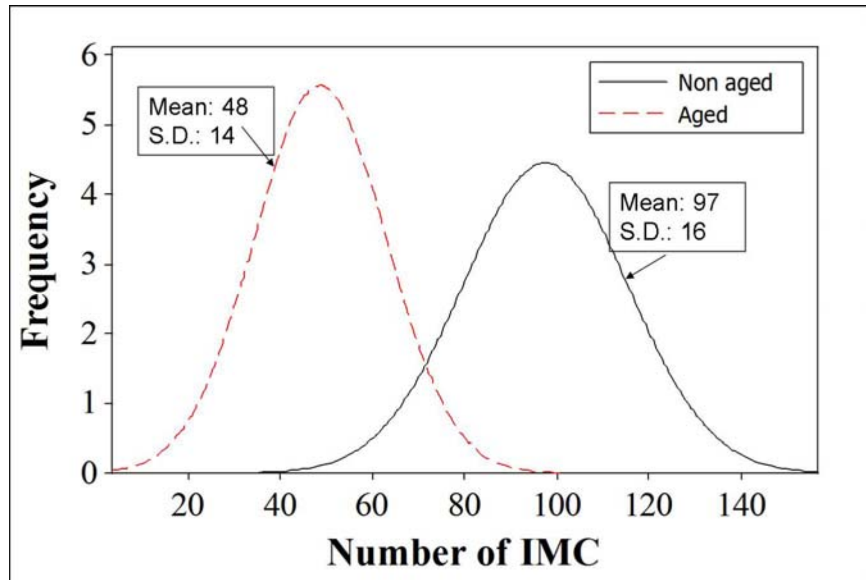


**Figure 48: Number of IMC in the bulk solder for aged and non-aged solder joints**

The reduction in the number IMC particles in aged solder joints appears to occur due to a reduction in smaller IMC particles and an increase in size of larger IMC

particles. A reduction in the amount of IMCs in aged solder joints is expected, since IMCs undergo phase coarsening with exposure to time and temperature, due to which smaller IMC particles combine with larger IMC particles. Coarsening occurs in accordance with Thompson-Freundlich solubility relationship [45], according to which concentration gradient exists between adjacent particles in a matrix. Concentration gradients in the matrix cause the particles to diffuse in the direction of the largest particles and away from the smallest particles. Consequently, phase coarsening causes small particles to combine with large particles. As the flow of particle proceeds, the small particles dissolve to compensate for the decrease in the concentration at their interface. This growth and dissolution process continues until the system is finally phase separated.

The increase in the size of IMC upon aging has been previously reported in well recognized Journal. Yang et al., [56] report that, upon isothermal aging intermetallics through out the joint coarsen and due to coarsening IMCs such as Cu6Sn5 in the bulk solder decrease in number and tend to increase in size. Deng et. al. [53] and Allen et al. [57] have also reported similar findings with the coarsening behavior of $Cu_6Sn_5$ IMC in the bulk solder. As the coarsening behavior is well documented it would not have been a unique contribution from this study. Therefore out of the two parameters; change in size and number of IMCs, I only quantified the change in the number of IMCs due to aging to baseline my work with previously reported literature.

From a fatigue reliability standpoint, the presence of IMC particles in the bulk solder may strengthen the tin grain boundaries and can retard crack propagation, while a reduction in the amount of IMC particles in the bulk solder may reduce fatigue resistance.

Consequently, crack propagation may be faster in aged solder joints than in non-aged joints thus resulting in a reduced reliability for aged solder joints.

In order to study the impact of grain growth and intermetallic particles on temperature cycle fatigue life, microstructural analysis was conducted on both non-aged and aged samples that were subjected to the temperature cycling test. Sample preparation was the same as previously discussed. For the lead-free solder interconnects, temperature cycling was found to increase the number of grains and grain boundaries. Figure 49 shows the image of tin grains near the cracked region where the failure occurred. Under temperature cycling, recrystallization appears to occur in regions of higher plastic deformation in lead-free solder interconnects. This recrystallization process results in a reduction in grain size and increase in the number of grain boundaries

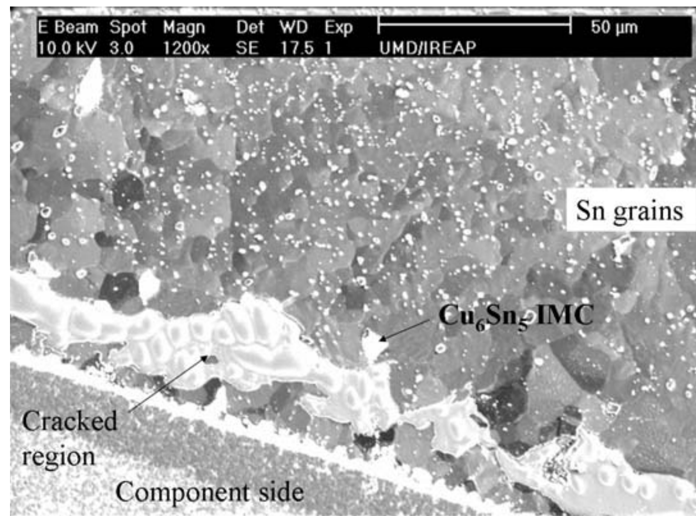


**Figure 49: Image of tin grains near the cracked region in a lead-free solder joint after temperature cycling.**

In tin-lead joints, phase coarsening occurs wherein tin and lead phases coarsen over time and facilitate grain boundary sliding. However with tin-silver-copper lead-free

solder, intermetallics such as $Cu_6Sn_5$ and $Ag_3Sn$ dispersed within the tin matrix (see Figure 49) appear to strengthen grain boundaries and restrict grain boundary sliding [58]. The failure in tin-silver-copper solders appears to be impacted by changes occurring to intermetallics present in grain boundaries in bulk solder.

The influence of IMC in tin-silver-copper solder failure is examined by analyzing the microstructure of three solder balls per BGA for two failed BGA components. In this investigation, solder cracks associated with electrical failure were found at the component side of the solder joint (see Figure 50) and in the solder joints near the die shadow region of the BGA components for both tin-lead and lead-free solder joints. This finding appears to be related to the smaller joint area at the component side as compared to the board side occurred.

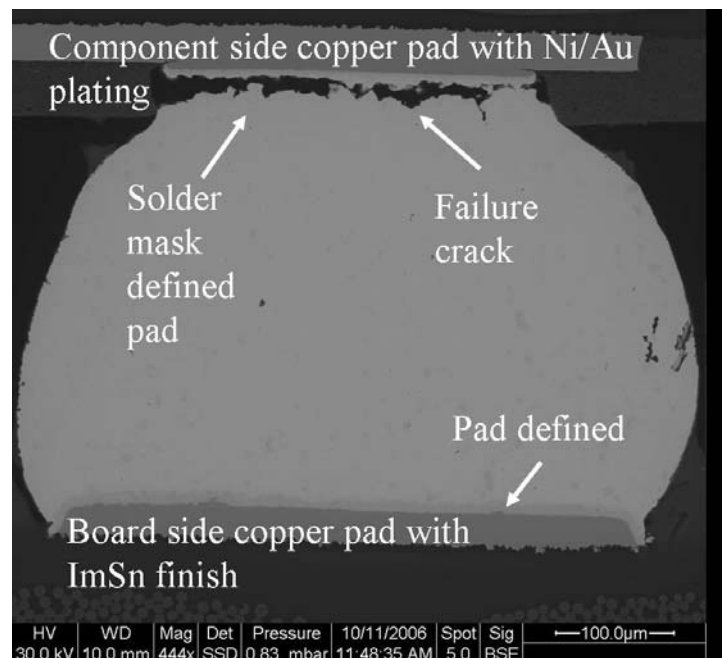


**Figure 50: Crack location for lead-free solder joint after thermal cycling.**

To more closely examine the grain structure along the crack path, the fracture site was prepared using focused ion beam (FIB). This analysis indicates that the crack path

occurred in the solder away form the intermetalic layer which formed between the metallization at the component pad and the solder. FIB images for all the solder joints analyzed showed the presence of small tin grains above and below the fracture site (see Figure 51).

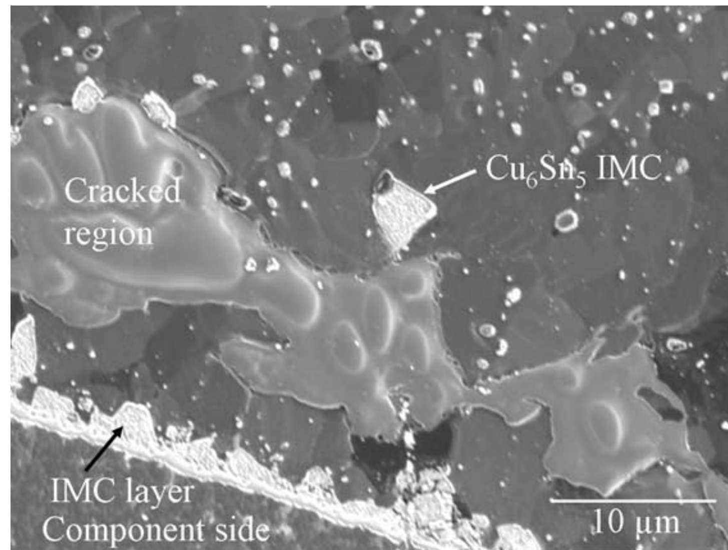


**Figure 51: Ion image from FIB showing crack location on the component side for lead-free solder joint (Image shows the presence of $Cu_6Sn_5$ IMC in the bulk solder)**

The reduced grain size along the crack path and location of the crack in the solder is also observed in solder joint that had not yet completely failed (see Figure 52). An electron microscopy image of the same location reveals a $Cu_6Sn_5$ IMC (see Figure 53). The presence of $Cu_6Sn_5$ intermetallic compounds at the grain boundaries is found as they tend to segregate along the grain boundaries during the solidification of tin grains [59].

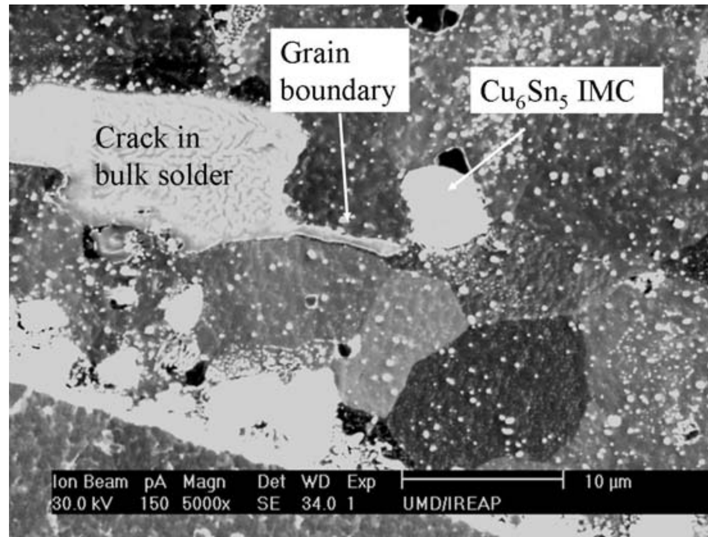


**Figure 52: Magnified ion image of crack path for lead-free solder joint**

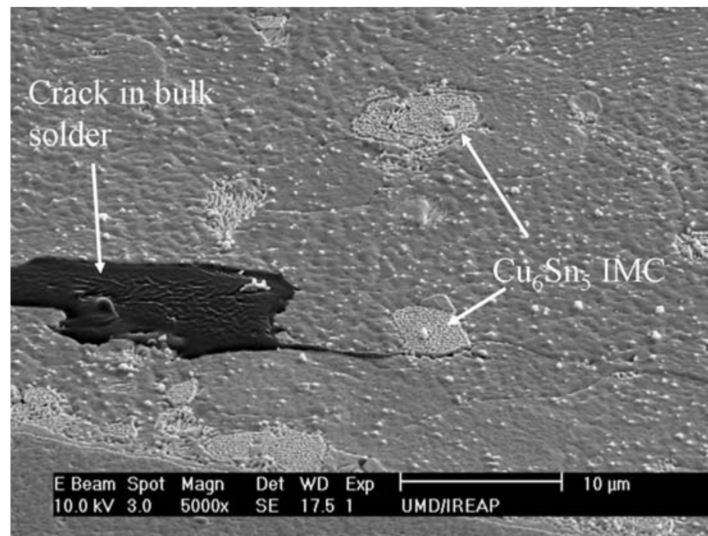


**Figure 53: Electron microscopy image showing the crack path for lead-free solder joint (crack tends to follow the pattern by passing along the grain boundaries)**

The microstructural analysis along solder crack paths revealed the presence of $Cu_6Sn_5$ and $Ag_3Sn$ IMCs (see Figure 54). In instances where the IMCs appeared in the crack path the crack deviated course around the IMC. Figure 54 shows the $Cu_6Sn_5$ and $Ag_3Sn$ intermetallic dispersed in the bulk solder near the crack and crack propagating around these IMCs. Higher number distinct $Cu_6Sn_5$ IMC particles were observed for non-

aged joint (see Figure 55) compared to aged solder joints. Grain size in aged and non-aged solder joints was found to be comparable after thermal cycling. IMC particles in the bulk solder coarsen over time which results in a decrease in the number of IMC particle in the solder.

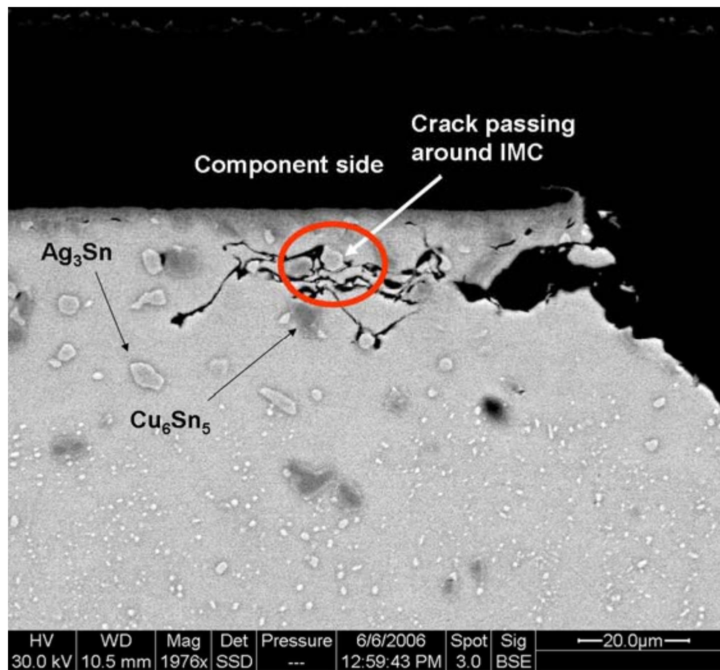


**Figure 54: SEM image showing crack passing around the IMC in bulk solder**

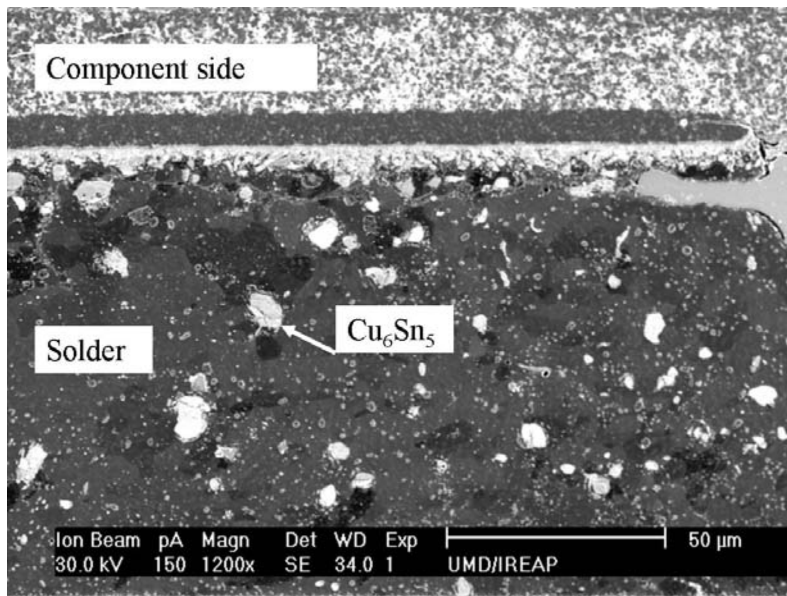


**Figure 55: Ion beam image of thermal cycled solder joint with no aging prior to thermal cycling**

### 5.5. Conclusions

The influence of the solder microstructure on temperature cycle fatigue life for solder interconnect was examined. The study included tin-lead and tin-silver-copper solders considering the impact of isothermal aging. A set of test specimens were subjected to 350 hour at 125$^{o}$C, while the other set remained un-aged. Temperature cycle fatigue life was determined by subjecting non-aged and aged test specimens to a -40 to 125$^{o}$C cycle. Solder interconnect fatigue failures identified by electrical continuity measurements during the temperature cycle test revealed that isothermal aging had a greater impact on tin-silver-copper solder interconnects compared to tin-lead. Statistical analysis of failure data showed a 25% reduction in characteristic life of aged tin-silver-copper interconnects as compared to non-aged joints. No significant difference was found between aged and non-aged tin-lead solder interconnects.

Microstructural analysis of non-temperature cycled lead-free solder interconnects found a reduction in the number of tin rich grains as well as a reduction in intermetallic particles as a result of isothermal aging. Microstructural analysis of temperature cycled solder interconnects found small re-crystallized grains along the crack path. For non-aged specimens, intermetallic particles were found to offer more obstructions to observed cracks as compared with aged specimens. The influence of intermetalic particle may also play a role in the wider failure distribution measured for the aged lead-free specimens as compared to the non-aged lead-free specimens. These particles may also in part explain the general wider failure distribution observed with tin-silver-copper solder as compared with tin-lead solder interconnects.

Microstructural changes occurring in lead-free solder joints as a result of environmental conditions such as storage at high temperatures for longer durations can affect the thermal fatigue reliability of lead-free solder joints. Aging conditions (125ºC for 350 hours) in this study represent an equivalent IMC formation after 10 years at 70ºC[60]. Thus, exposure to storage conditions at high temperatures for longer duration would lead to degradation in lead-free solder joint reliability.

# Chapter 6: PULL STRENGTH TEST

## 6.1. Theory

QFP components are one of the widely used components in electronics assembly. These components have terminals which are J-lead or gull wing shaped. They provide superior thermal fatigue performance compared to BGA components but have limited number of input output terminals compared to BGA components [1]. Due to their longer fatigue life, testing for thermal fatigue becomes a time consuming effort. In order to minimize the time, pull test of leads for QFP components has been widely accepted in the industry as a standard test for solder joint strength of QFP components [62]. In this study, solder joint strength analysis will include the influence of aging on the joint strength for various metallurgical combinations.

## 6.2. Design of experiment

In this study, QFP components, with copper lead frame, assembled with various solders, board pad finishes, and lead finishes were analyzed. The Pb-free QFP lead finishes included Sn, Sn0.7Cu and Sn2Bi. They were soldered on polyimide (PI) and FR-4 boards (see Figure 56) with Cu pads plated with ENIG, ImAg, HASL, OSP and ImSn finish. Components were soldered with Sn37Pb, Sn3.5Ag and Sn3.0Ag0.5Cu solders. Material combinations of the specimens are listed in Table 9 and Table 10. Lead pull tests were conducted to evaluate the solder joint strength. Isothermal aging effects on solder joint strength were investigated after specimens were exposed to 350 and 1000 hours aging at 125ºC. Cut-out features [61] were designed in the boards to be able to remove

components for analysis without disturbing the adjacent components. Figure 57 shows the QFP component removed from the board assembly on which the pull test was conducted. Figure 58 shows the cross-sectional schematic of the QFP component.

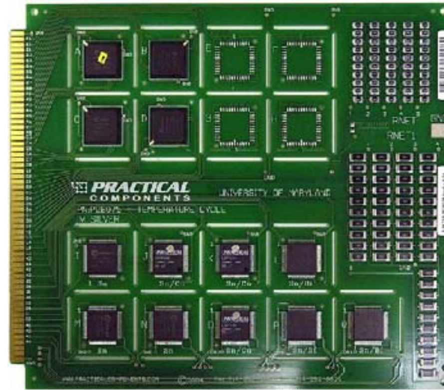


**Figure 56: Printed circuit board**

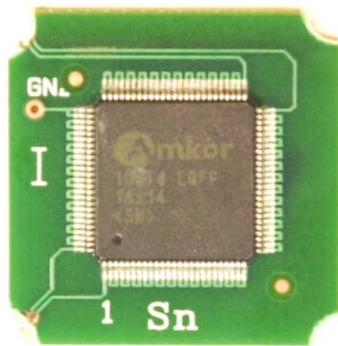


**Figure 57: Cutout QFP package assembly**

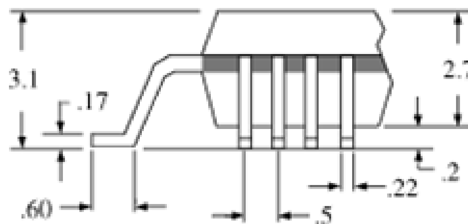


**Figure 58: QFP package dimensions (mm)**

**Table 9: Interconnect assembly configuration – FR4 boards**

| Configuration | Component lead finish | Solder paste | Pad finish |
|---|---|---|---|
| SnPb | Sn10Pb | Sn37Pb | HASL |
| Pb-free | Sn, Sn0.7Cu, Sn2.0Bi | Sn3.0Ag0.5Cu | ImSn |
| | | | ImAg |
| | | | ENIG |
| | | | OSP |

**Table 10: Interconnect assembly configuration - PI boards**

| Configuration | QFP lead finish | Solder paste | Pad finish |
|---|---|---|---|
| Pb-free | Sn, Sn0.7Cu, Sn2.0Bi | Sn3.0Ag0.5Cu | ImSn |
| | | | ImAg |
| | | | ENIG |
| Pb-free | Sn, Sn0.7Cu, Sn2.0Bi | Sn3.5Ag | ImSn |
| | | | ImAg |
| | | | ENIG |

To determine the solder joint strength pull test was conducted by pulling individual leads. A test fixture was designed and fabricated to conduct the lead pull test. The fixture was designed such that the sample was placed at an angle of 45º with the horizontal plane [62]**.** Test was performed using DAGE 4000 pull tester. Sample was mounted on the fixture and placed on the pull tester stage. A copper hook from the tester pulls the lead and the highest force at which the break occurs is recorded for each pull strength test. The pull rate used in this study was 166 µm/sec because it satisfied the standard [62] and precipitated failures in the solder joint. A schematic view of the sample orientation is shown in Figure 59. Forty leads (10 consecutive leads on each side) from each QFP were pulled. The failure mode was recorded for each test and only the pull strength data corresponding to solder joint failure were considered for solder joint strength analysis.

Analysis was performed to understand the effect of pull rate on the failure mode (solder joint failure, pad peel off), to determine the pull strength and to make comparative analysis. It was observed that, at a speed < 300 μm/sec, failures were mostly solder joint fractures; at a rate > 300 μm/sec, the potential for pad failures increases.

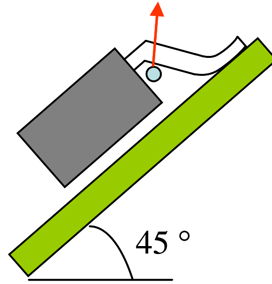


**Figure 59: Sample orientation schematic.**

### 6.3. Test results

Figure 60 shows the effect of aging on solder joint strength for various pad finishes for QFP having Sn plated leads attached onto FR4 board with Sn3.0Ag0.5Cu solder. For comparison, strength results for QFP having SnPb coated leads attached with SnPb solder on HASL pad finish have also been plotted and is represented as HASL-SnPb. Results indicate that the maximum reduction in solder joint strength (14% reduction) after 1000 hours of aging occurred for ENIG pad finish and the least reduction occurred for ImSn pad finish among the Pb-free pad finishes. SnPb solder joints showed 19% degradation in the strength after 1000 hours of aging which was greater than the strength degradation experienced by Pb-free solder joints.

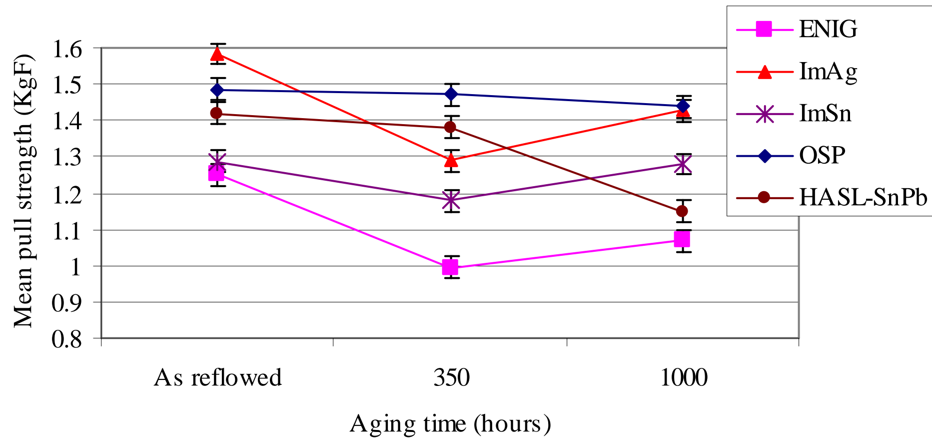


**Figure 60: Effect of aging on pull strength for Sn3.0Ag0.5Cu solder with Sn lead finish with ENIG, ImSn, ImAg and OSP pad finish on FR4 board. Pull strength results are also shown for assemblies with SnPb lead finish attached with SnPb solder on HASL pad finish represented by HASL-SnPb**

Analysis of the fracture surface was conducted to understand the lower solder joint strength associated with ENIG pad finish. Elemental analysis on the fracture surface at the pad side shown in Figure 61 was conducted using Energy dispersive X-ray (EDX) to determine the composition of fracture surface. Results (see Table 11) showed the ratio of (NiCu):Sn to be (45.67): 52.9 which is indicative of $(NiCu)_3Sn_4$ IMC for pads with ENIG finish. For ImAg finish pads, Cu: Sn ratio was found to be 54.65:45.36 which is indicative of $Cu_6Sn_5$ IMC. One of the parameter involved in the fracture of solder joint is the toughness which is indicative of the resistance to fracture of a material under stress. Literature [63] has reported the toughness values for $Ni_3Sn_4$ to be 1.2 ($MPa.m^{-1/2}$) which is lower than the toughness value for $Cu_6Sn_5$ IMC, which is 1.4 ($MPa.m^{-1/2}$). From the toughness values, fracture can be expected to occur at the $(NiCu)_3Sn_4$ IMC layer prior to $Cu_6Sn_5$ IMC.

Solder joints for the ImAg and ENIG pad finish were then cross-sectioned to examine the failure site. It was found that for ENIG pad finish fracture occurred at the

pad interface (Figure 62) where $(NiCu)_3Sn_4$ IMC were detected whereas for ImAg pad finish, the fracture was between the lead and the solder interface (Figure 63) where the $Cu_6Sn_5$ IMC was detected.

**Table 11: Atomic % of elements at the fracture surface for QFP(Sn) - Sn3.0Ag0.5Cu Solder - Aged at 125ºC for 350 hrs for pad with ImAg and ENIG finish**

| Element | ENIG | ImAg |
|---|---|---|
| Sn | 52.9 (± 0.47) | 45.36 (± 0.83) |
| Cu | 42.03 (± 0.34) | 54.65 (± 0.74) |
| Ni | 3.64 (± 0.15) | None |
| Au | 1.43 (±0.34) | None |

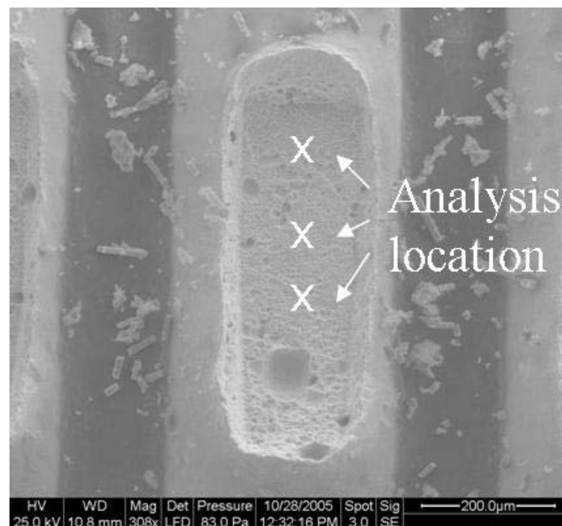


**Figure 61: Fracture surface on pad side for QFP (Sn) - Sn3.0Ag0.5Cu solder - ENIG pad finish sample, Aged at 125C for 350 hours where the elemental analysis was conducted**

**Figure 62: Cross-sectional view of fracture surface for QFP (Sn) - Sn3.0Ag0.5Cu solder - ENIG pad finish sample, Aged at 125C for 350 hours – Fracture site found to be at the IMC**

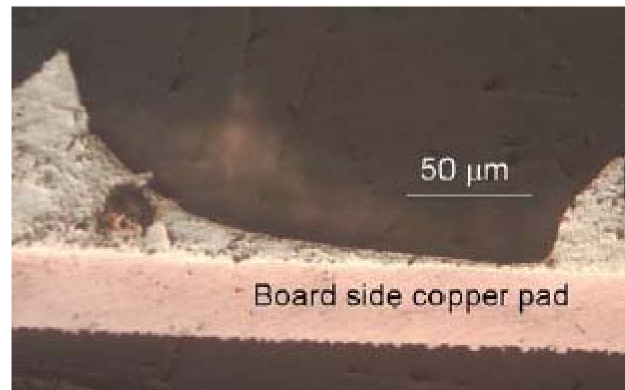


**Figure 63: Cross-sectional view of fracture surface for QFP (Sn) - Sn3.0Ag0.5Cu solder - ImAg pad finish sample, Aged at 125C for 350 hours – Fracture site between the lead and solder interface**

Figure 64 shows the effect of aging on solder joint strength for various pad finishes for QFP having SnCu plated leads attached onto FR4 board with Sn3.0Ag0.5Cu solder. Results indicate that the maximum degradation in solder joint strength (20% reduction) after 1000 hours of aging occurred for ImAg pad finish and the least degradation occurred for ImSn pad finish.

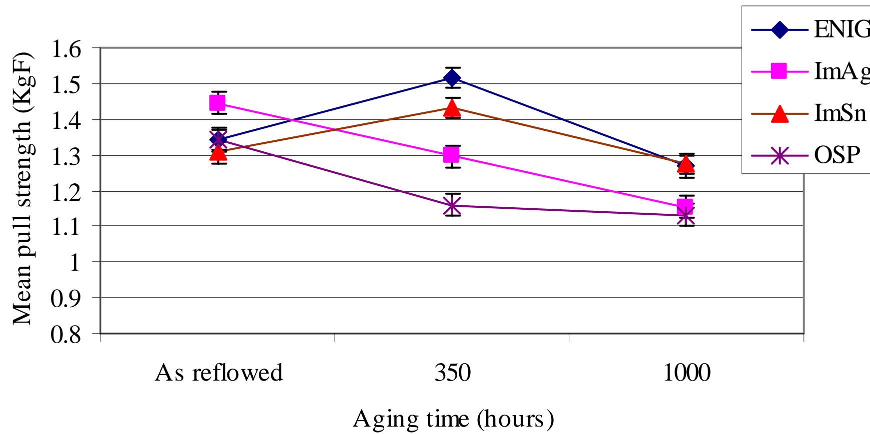


**Figure 64: Effect of aging on pull strength for Sn3.0Ag0.5Cu solder with SnCu lead finish with ENIG, ImSn, ImAg and OSP pad finish on FR4 board**

Figure 65 shows the effect of aging on solder joint strength for various pad finishes for QFP having SnBi plated leads attached onto FR4 board with Sn3.0Ag0.5Cu solder. Results indicate that the maximum degradation in solder joint strength (10% reduction) after 1000 hours of aging occurred for ENIG pad finish and the least degradation occurred for ImSn and ImAg pad finish.

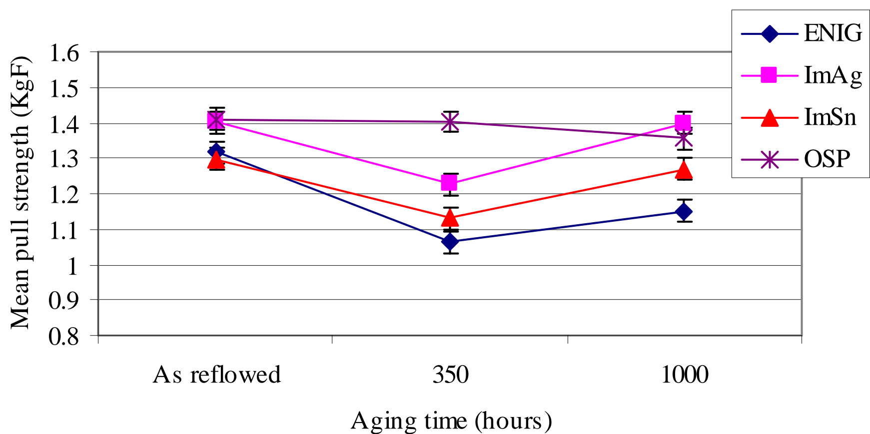


**Figure 65: Effect of aging on pull strength for Sn3.0Ag0.5Cu solder with SnBi lead finish with ENIG, ImSn, ImAg and OSP pad finish on FR4 board**

Further data analysis was conducted using the full factorial design to analyze the results and determine the influence of lead finish, pad finish and aging time on the solder

joint strength. Data analysis consisted to three factors, aging conditions, pad finishes and lead finishes, with three levels (As reflowed, 350 hrs and 1000 hrs) for aging conditions, four levels for pad finish (ENIG, ImAg, ImSn, OSP) and three levels for lead finish (Sn, SnCu, SnBi) for FR4 boards. Levels for PI boards consisted of three levels (As reflowed, 350 hrs and 1000 hrs) for aging conditions, three levels for pad finish (ENIG, ImAg, ImSn) and three levels for lead finish (Sn, SnCu, SnBi). In this analysis, all the data corresponding to the factor under study are grouped into levels. For example, to study the effect of aging on pull strength, the data for each pad finish and lead finish were grouped according to the levels of aging, i.e., the data for as-reflowed will consist of as-reflowed results from all the pad finishes and lead finishes.

Figure 66 shows the effects of aging on the solder joint strength for Sn3.0Ag0.5Cu solder on FR4 board. Results indicate a 10 % reduction in solder joint strength for Sn3.0Ag0.5Cu solder joints after 350 hours of aging, aging after 350 hours has negligible effect on solder joint strength. Based on these results a qualification test to assess solder joint strength degradation can be terminated at 350 hours as there is insignificant reduction in strength after 1000 hours.  This can lead to cost reduction in qualification testing of electronic assemblies.

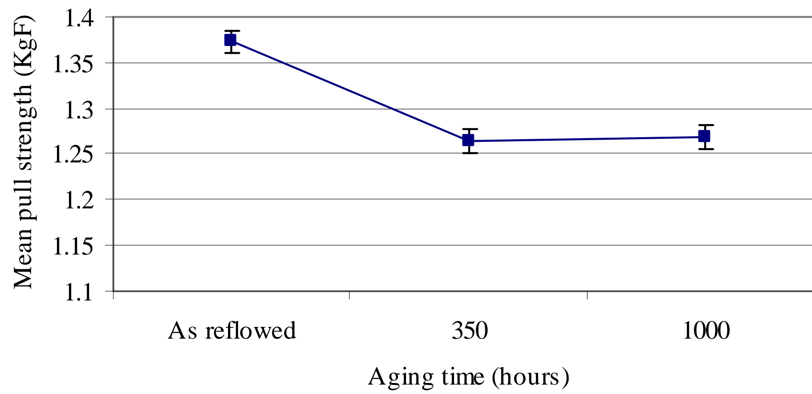


**Figure 66: Effect of aging on pull strength for Sn3Ag0.5Cu solder on FR4 board**

Figure 67 shows the effects of pad finish on the solder joint strength for Sn3.0Ag0.5Cu solder on FR4 board. Solder joints with ENIG pad finish had the lowest solder joint strength and those with ImAg pad finish had the highest strength. Figure 68 shows the effects of lead finish on the solder joint strength for Sn3.0Ag0.5Cu solder on FR4 board. Results indicate that lead finish doesn’t have a significant influence on solder joint strength.

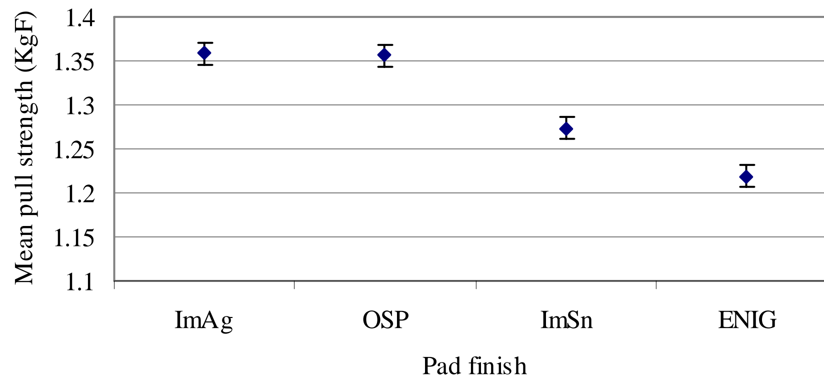


**Figure 67: Effect of pad finish on pull strength for Sn3Ag0.5Cu solder on FR4 board**

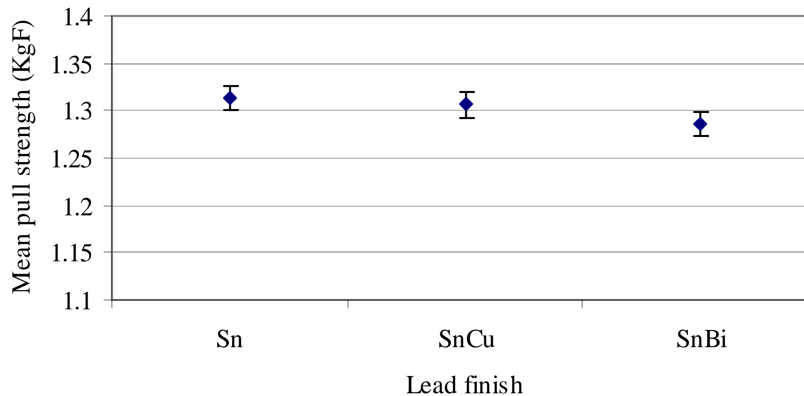


**Figure 68: Effect of lead finish on pull strength for Sn3Ag0.5Cu solder on FR4 board**

Figure 69 shows the effect of aging on pull strength for a SnPb assembly (SnPb QFP – SnPb solder paste), mixed - SnPb (Pb-free QFP- SnPb paste) and pure Pb-free (Pb-free QFP- Sn3Ag0.5Cu paste) assemblies. Figure 70 and Figure 71 show the effect of pad finish, and lead finish on pull strength for pure Pb-free and mixed assemblies. Results show that aging reduces the solder joint strength for pure SnPb, pure Pb-free, and mixed assemblies. For pure Pb-free assemblies, aging after 350 hours has a negligible effect, whereas for SnPb and mixed assemblies, pull strength is adversely affected even after

350 hours. Until 350 hours of aging, pure SnPb assembly shows a 5 percent higher pull strength than pure Pb-free, and the pull strength for pure Pb-free is 2 percent higher than that of mixed assemblies.

It was found that, for ENIG pad finish, pure Pb-free assembly shows a 7 percent higher pull strength than mixed assemblies. In terms of lead finish, mixed assemblies showed higher pull strength for Sn and SnCu lead finishes, whereas for SnBi, a pure Pb-free solder joint has higher pull strength.

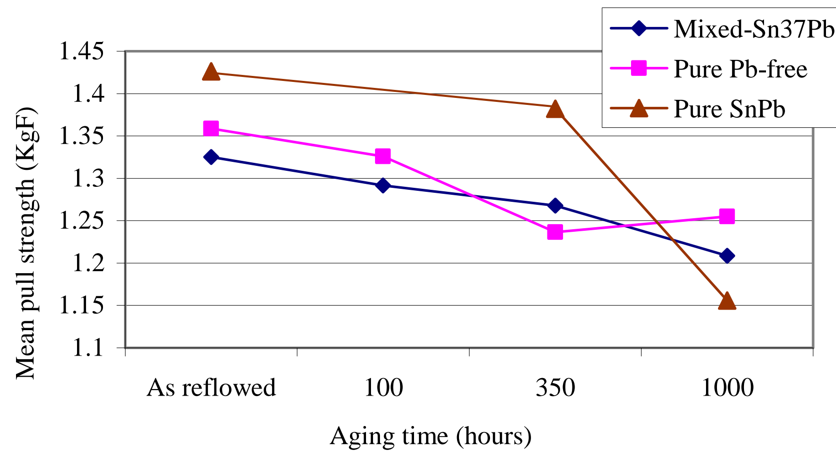


**Figure 69: Effect of aging on pull strength for Mixed - SnPb (Pb-free QFP- SnPb paste), Pure Pb-free (Pb-free QFP- Sn3Ag0.5Cu paste) and Pure SnPb (SnPb QFP- SnPb paste) assemblies**

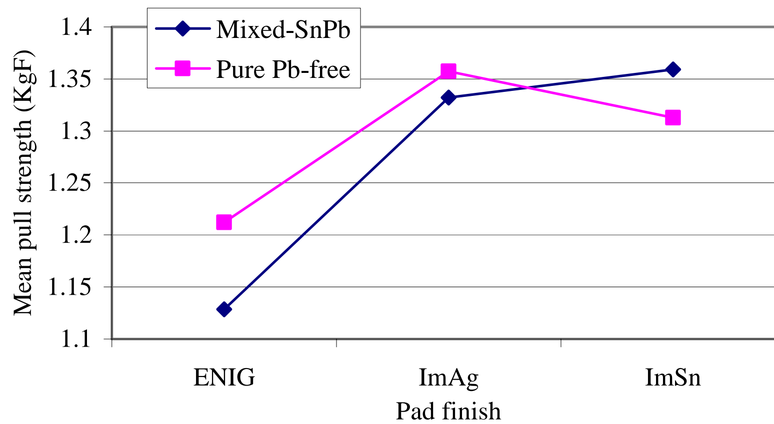


**Figure 70: Effect of pad finish on pull strength for Mixed –SnPb (Pb-free QFP-SnPb paste), Pure Pb-free (Pb-free QFP- Sn3Ag0.5Cu paste)**

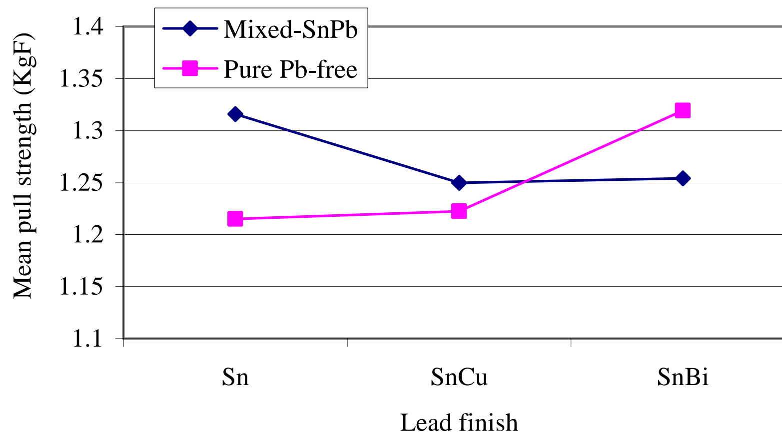


**Figure 71: Effect of lead finish on pull strength for Mixed –SnPb (Pb-free QFP-SnPb paste), Pure Pb-free (Pb-free QFP- Sn3Ag0.5Cu paste)**

### 6.4. Conclusions

This study was conducted to assess thermal aging effects on the solder joint strength of QFP components assembled with Pb-free (Sn3.5Ag and Sn3.0Ag0.5Cu) solders. It was observed that high-temperature aging reduces the solder joint strength for both solder assemblies till 350 hours. Excessive aging after 350 hours has minor effect on solder joint strength.

It was found that, Sn3.0Ag0.5Cu solder joint strength is approximately 15% higher than Sn3.5Ag solder joints. For both Sn3.5Ag and Sn3.0Ag0.5Cu solder joints, pad finish has a significant effect on solder joint strength. ImAg and OSP pad finishes offer higher strength than other finishes; whereas, the ENIG finish resulted in the weakest joint. Analysis of fracture surface indicated the presence of $(NiCu)_3Sn_4$ IMC for ENIG pad finish where as $Cu_6Sn_5$ IMC for ImAg pad finish. Due to the lower toughness value of $(NiCu)_3Sn_4$ the fracture occurred at IMC layer on the pad side for ENIG pad finish whereas due to the absence of Ni in ImAg pad finish the fracture occurred at the $Cu_6Sn_5$ IMC layer between the lead and solder.

In terms of lead finish, although SnBi lead finish provided higher strength than Sn and SnCu lead finishes for Sn3.0Ag0.5Cu solder joints in PI board assemblies, lead finish tends to have little effect on solder joint strength.

The pull strengths for mixed solder and pure SnPb solder assemblies' decrease monotonically with aging, even after 350 hours, whereas for pure Pb-free joints the effect of aging is negligible after 350 hours. Until 350 hours of aging, a pure SnPb assembly shows a 5 percent higher pull strength than pure Pb-free, and the pull strength for a pure Pb-free assembly is 2 percent higher than for mixed assembly.

In terms of the effect of the pad finish on pull strength, an ENIG pad finish in a pure Pb-free assembly shows a 7 percent higher pull strength than in mixed assemblies. In terms of lead finish, mixed assemblies showed higher pull strength for tin and tin-copper lead finishes, whereas for tin-bismuth, a pure Pb-free solder joint has higher pull strength.

# CONTRIBUTIONS

Due to the lead-free transitions, intense research is ongoing in investigating the reliability of solder joint formed by lead-free materials. In particular, research is being conducted to assess new solder paste alloys, printed circuit board finishes and component terminal metallization. Along with the concerns related to lead-free materials, mixing of Pb in lead-free assembly is becoming a concern for industries exempt from lead-free legislation.

Metallurgies present at the component terminal, printed circuit board and solder alloy make up the microstructure of solder joint. During operation and storage, solder joint reliability degrades due to the changes occurring in the solder joint microstructure over time. A fundamental understanding is required to study the microstructural changes in lead-free, SnPb and mixed solder joints and their influence of solder joint reliability.

The specific contributions of this research include the determination of microstructural features those undergo changes over time when exposed to environmental thermal conditions and their influence on thermal fatigue reliability of solder joints.

It was demonstrated that microstructure of lead-free solder joints consists of $Cu_6Sn_5$ and $Ag_3Sn$ IMC in the bulk solder. On the component side, IMCs such as $(Ni,Cu)_3Sn_4$, $(Cu,Ni)_6Sn_5$ and $(Au,Ni)Sn_4$ IMC were found at the interface between solder to copper pad with Ni/Au finish after long term isothermal aging for 1000 hrs at 125ºC. On the board side, $Cu_6Sn_5$ and $Cu_3Sn$ IMC were found in case of ImSn, ImAg and OSP finish and $Ni_3Sn_4$ IMC in case of ENIG finish after long term isothermal aging for 1000 hrs at 125ºC. It was determined that, though long term aging may create several IMCs at

the solder to copper pad interface, IMCs present in the bulk solder such as $Cu_6Sn_5$ play a key role in governing time to failure in thermal fatigue.

Thermal fatigue failures were found in the bulk solder and fatigue crack was found to propagate intergranularly between Sn grains. $Cu_6Sn_5$ were found distributed in solder joints at Sn grain boundaries and were demonstrated to influence crack propagation in thermal fatigue by being present as obstructions to crack propagation. Demonstrated that isothermal aging for 350 hrs at 125ºC causes coarsening of $Cu_6Sn_5$ IMC in the bulk solder and results in 50% reduction in number of IMCs in the bulk solder, thus promoting the crack to propagate faster along the grain boundary. This dissertation determined that isothermal aging for 350 hrs at 125ºC would cause a 25% reduction in characteristic life for lead-free solder joints with ImSn pad finish. Environment storage conditions would affect thermal fatigue reliability of lead-free solder joints.

Determined that mixed solder joints are not prone to Pb phase coarsening under long term aging for 350 hrs at 125ºC as opposed to SnPb solder joints wherein Pb phase undergoes coarsening. Resistance to Pb coarsening would results in mixed solders to have better thermal fatigue life than SnPb solders and have been reported by several studies [11][14][16].

Demonstrated that the presence of Pb in mixed solder results in 30 to 40% lower IMC thickness compared to Pb-free and SnPb solder joints by being present at the interface as a diffusion barrier between Ni and Sn for IMC formation. Less IMC would results in mixed solders being better fatigue resistant in high stress loading such as

vibration and shock where failures occur at IMC. Determined that solder joint strength for mixed solder joints are comparable to SnAgCu for all the pad finishes and lower than SnPb solder joints in high stress test such as pull test.

# REFERENCES


[1] Ganesan S. and Pecht M., "Lead-free Electronics", John Wiley and Sons Inc., New York, New York 2006

[2] Pecht, M., Fukuda Y., and Rajagopal S., "The Impact of Lead-free Legislation Exemptions on the Electronics Industry", IEEE Transactions on Electronics Packaging Manufacturing, Vol. 27, No. 4, pp. 221-232, October 2004.

[3] Ciocci, R., and Pecht M., "Questions Concerning the Migration to Lead-free Solder", Circuit World, Vol. 30, No. 2, pp. 34-40, 2004.

[4] Fukuda, Y., Casey P., and Pecht M., "Evaluation of Selected Japanese Lead-free Consumer Electronics", IEEE Transactions on Electronics Packaging Manufacturing, Vol. 67, No. 4, pp. 305-312, October 2003.

[5] Fukuda, Y., Pecht M., Fukuda K., and Fukuda S., "Lead-free Soldering in the Japanese Electronics Industry", IEEE Transactions on Components and Packaging Technologies, Vol.26, No.3, pp. 616-624, September 2003.

[6] Dasgupta A., Sharma P. and Upadhyayula, "Micro-mechanics of fatigue damage in Pb-Sn solder due to vibration and thermal cycling", International Journal of Damage Mechanics, Vol. 10, pp. 101-132, April 2001

[7] Basaran C. and Wen Y., "Grain growth in eutectic Pb/Sn ball grid array solder joints", Inter society conference on thermal phenomena, pp. 903-908, 2002

[8] Choubey A., Wu J., Ganesan S., and Pecht M., "Lead-Free Assemblies in High Temperature Applications", Proceeding of IMAPS International Conference on High Temperature Electronics (HITECH 2006), May 2006.

[9] Choubey A., Menschow D., Ganesan S., and Pecht M., "Effect of Aging on Pull Strength of SnPb, SnAgCu and Mixed Solder Joints in Peripheral Surface Mount Components" Journal of Surface Mount Technology Association, April 2006.

[10] Wu J. and Ganesan S., "Using cut-out features for efficient printed circuit board testing and failure analysis", IEEE transactions on component and packaging technology, vol. 28, issue 1, pp. 166-168, March 2005

[11] Hua F., Aspandiar R., Rothman T., Anderson C., Clemons G. and Klier M., "Solder joint reliability of SnCuAg BGA components attached with eutectic SnPb solder paste, Journal of Surface Mount Technology Association, vol. 16, Issue 1, 2003.

[12] Hillman D., Wells M., Cho K., "The impact of reflowing a Lead-free solder alloy using a SnPb solder alloy reflow profile on solder joint integrity", Proceedings of International Conference on Lead-free Soldering, Ontario, Canada, May 24-25, 2005.

[13] Grossmann G., Tharian J, Jud P, Sennhauser U., "Microstructural investigation of lead-free BGAs soldered with tin-lead solder", Soldering and Surface Mount Technology, Vol. 17, No. 2, pp. 10-21, Feb. 2005

[14] Hillman D. and Wilcoxon R., "JCAA/JG-PP No-Lead Solder Project:-55ºC to +125ºC Thermal Cycle Testing Final Report", March 15, 2006

[15] Chalco P., "Solder fatigue reliability issues in lead-free BGA packages", Pan Pacific Symposium, 2002.

[16] Nelson D., Pallavicini H., Zhang Q., Friesen P., and Dasgupta A., "Manufacturing and reliability of Lead-free and mixed system assemblies

(SnPb/Lead-free) in avionics", Journal of Surface Mount Technology Association, vol. 17, issue 1, 2004.

[17] Chung C.K., Aspandiar R., Leong K.F. and Cheng S. T., "The interactions of lead (Pb) in lead-free solder (Sn/Ag/Cu) system", Electronic component and technology conference, pp. 168-175, 2002.

[18] Zeng X., "Thermodynamic analysis of influence of Pb contamination on Lead-free solder joints reliability", Journal of Alloys and Compounds, Vol. 348, No. 1, pp. 184-188, January 2003.

[19] Chang L., Huang Z., Conway P. and Thompson R., "Materials behavior and intermetallics characteristics in the reaction between SnAgCu and SnPb solder alloys", Proceedings of Electronic Component and Technology Conference, pp. 1347-1353, Las Vegas, Nevada, June 1-4, 2004.

[20] Choi S., Bieler T.R., Subramanian K.N. and Lucas J.P., "Effect of Pb contamination on the eutectic Sn-Ag solder joint", Soldering and Surface Mount Technology, vol. 13, issue 2, pp. 26-29, April 2001.

[21] Oliver J., Nylen M., Rod O. and Markou C., "Fatigue properties of Sn3.5Ag0.7Au solder joints and effects of Pb-contamination", SMTAI conference proceedings, 2002

[22] Zhu Q., Sheng M. and Luo L., "The effect of Pb contamination on the microstructure and mechanical properties of SnAg/Cu and SnSb/Cu solder joints in SMT", Soldering and Surface Mount Technology, vol. 12, Issue 3, pp. 19-24, March 2000.

[23] Snugovsky P., Zbrzezny A.R., Kelly M., Romansky M., "Theory and practice of lead-free BGA assembly using Sn-Pb solder", Proceedings of International Conference on Lead-free Soldering, Ontario, Canada, May 24-25, 2005.

[24] Seelig K. and Suraski D., "Lead contamination in lead-free electronics assembly", Technical publication AIM

[25] Kalssen M. and Cahoon J.R., "Interdiffusion of Sn and Pb in liquid Pb-Sn alloys", Metallurgical and Materials Transactions A, vol. 31A, pp. 1343-1351, May 2000

[26] http://www.metallurgy.nist.gov/phase/solder/solder.html, Phase Diagrams and Computational Thermodynamics, Accessed July 5th 2005.

[27] Ministry of Information Industry of the People's Rebublic of China, "Adminstrative Measure on the Control of Pollution Caused by Electronic Information Products", March 2006, [Online], http://www.graspllc.com/China%20RoHS.php, Accessed 04/09/06

[28] "RoHS Regulations: Government Guidance Notes 2007", URN 07/635, pp. 1-31, January 2007, [Online], http://www.dti.gov.uk/files/file37219.pdf, Accessed 04/09/07

[29] .Zhang Q., A. Dasgupta, and P. Haswell, "Creep and High-Temperature Isothermal Fatigue of Pb-free Solders", Proceedings of IPACK03, International Electronic Packaging Technical Conference and Exhibition, pp.1-6, July 6-11, 2003, Maui, Hawaii, USA.

[30] Li G.Y. and Chen B.L., “Formation and Growth Kinetics of Interfacial Intermetallics in Pb-free Solder Joints”, IEEE Transactions on Components and Packaging Technologies, Vol. 26, No. 3, pp. 651-658, September 2003.

[31] Zheng, Y., C. Hillman, and P. McCluskey, “Intermetallic Growth on PWBs Soldered with Sn3.8Ag0.7Cu”, Proceedings of the 52nd Electronic Components & Technology Conference, pp. 1226-1231, San Diego, 2002b.

[32] Luhua Xu, Pang J.H.L, Kithva H. P. and Low T.H., “Isothermal and thermal cycling aging on IMC growth rate in lead-free and lead based solder interface”, IEEE Transactions on Components and Packaging Technologies, Vol. 28, No. 3, pp. 408-414, Sep. 2005.

[33] Lee K.Y., Ming L., Olsen D.R., Chen W.T., Tan B.T.C. and Mhaisalkar S., “Microstructure, Joint Strength and Failure Mechanism of Sn-Ag, Sn-Ag-Cu versus Sn-Pb-Ag Solders in BGA Packages”, Proceedings of the 51st Electronic Components & Technology Conference, pp. 478-485, Orlando, FL, May 29th to June 1st, 2001.

[34] NIST, Phase diagrams and computational thermodynamics, http://www.metallurgy.nist.gov/phase/solder/solder.html Accessed 06/03/2006

[35] Tz-Cheng Chiu, Zeng K., Stierman R. and Edwards D., Ano K., “Effect of Thermal Aging on Board Level Drop Reliability for Pb-free BGA Packages”, Proceedings of Electronic Components and Technology Conference, pp. 1256-1262, June, 2004

[36] Borgesen P., “Fragility of Pb-free solder joints on Cu pads”, Research proposal Phase I, October 17th, 2004, UIC, Binghamton, N.Y.

[37] Roepsh J.A., Champaign R.F. and Downey M.R., “Case study: The effect of severe black pad defect on solder bonds on ball grid array components”, Journal of Surface Mount Technology, Vol. 15, Issue 3, pp. 19-24, 2002

[38] Coyle R.J., Popps D.E.H., Mawer A., Cullen D.P. Wenger G.M. and Solan PP., “The Effect of Modifications to the Nickel/Gold Surface Finish on Assembly Quality and Attachment Reliability of a Plastic Ball Grid Array”, IEEE Transactions on Components and Packaging Technologies, Vol. 26, No. 4, pp. 724-732, December 2003.

[39] Handwerker C., “Transitioning to Pb-free Assemblies”, Printed Circuit Design and Manufacture, pp. 17-23, March 2005.

[40] Dasgupta A., Sharma P. and Upadhyayula, “Micro-Mechanics Of Fatigue Damage in Pb-Sn Solder Due To Vibration And Thermal Cycling”, International Journal of Damage Mechanics, Vol. 10, pp. 101-132, April 2001

[41] Vianco, P., “An Overview of Surface Finishes and Their Role in Printed Circuit Board Solderability and Solder Joint Performance,” Circuit World, Vol. 25, No. 1, pp. 6-24, 1998.

[42] Tu P. L., Chan Y.C., Hung K.C., Lai J.K.L., “Study of micro-BGA solder joint reliability”, Microelectronics Journal, Vol. 41, No. 2, pp. 287-293, 2001

[43] McCormick H., Snugovsky P., Bagheri Z., Bagheri S., Hamilton C., Riccitelli G. and Mohabir R., “Mixing Metallurgy: Reliability of SAC Balled Area Array Packages Assembled using SnPb Solder”, Journal of Surface Mount Technology Association, vol. 20, Issue 2, pp. 11-18, 2007.

[44] Brandes E.A., Brook G.B., “Smithells Metals Reference Book”, Table 13.2, pp. 13-24, 7th Edition, 1992, Published by Butterworth Heinemann, Oxford, U.K.

[45] Sridhar, K., M. Glicksman S. Mani., and V. Fradkov, “Investigation of Microstructural Coarsening in SnPb Alloys,” Metallurgical and Materials Transactions A, Vol. 30A, pp. 1541-1549, June 1999.

[46] Frear D. R., “Thermomechanical Fatigue of Solder Joints: A New Comprehensive Test Method”, IEEE Transactions on Components, Hybrid and Manufacturing Technology, Vol. 12, No. 4, pp. 492-501, Dec 1990

[47] Lau J, Shangguan D., Castello T., Horsley R., Smetana J., Hoo N., Dauksher W., Love D., Menis I., Sullivan B.,“ Failure Analysis of Pb-free Solder Joints for High Density Packages”, Soldering and Surface Mount Technology, Vol 16, Issue 2, pp. 69-76, 2004

[48] Morris Jr. J.W., Tribula D., Summers T.S.E and Grivas D., “The Role of Microstructure in Thermal Fatigue of Pb/Sn Solder Joints”, Solder Joint Reliability, Von Nostrand Reinhold, New York, pp. 225-265, 1991

[49] Tu K.N., Lee T.Y., Jang J.W., Li L., Frear D.R., Zeng . and Kivilahti J.K., “Wetting Reaction Versus Solid State Aging of Eutectic SnPb on Cu”, Journal of Applied Physics, Vol. 89, No. 9, pp. 4843-4849, May 2001.

[50] Liu Y., Gale S., Johnson W.R., “Investigation of the Role of Void Formation at the Cu-to –Intermetallic Interface on Aged Drop Test Performance”, IEEE Transactions on Electronic Packaging Manufacturing, Vol. 30, No. 1, pp. 63-73, Jan 2007

[51] Bartelo, J., Henderson, D., Knadle, K., Sarkhel, A., Woods, J., Thiel, G., Caletka, D., Darbha, K., King, D., Woychik, C., Gosselin, T., Shih, D., Kang, S., Cain, S., and Puttlitz, K., "Thermomechanical Fatigue Behavior of Selected Lead-free Solders," Proc IPC / SMEMA Council APEX 2001 Conf, San Diego, CA, Jan. 14-18, 2001, pp. LF2-2-1 through LF2-2-12.

[52] Osterman M., Dasgupta A. and Han B., "A Strain Range Based Model for Life Assessment of Pb-free SAC solder Interconnects", Proceedings of the 56th Electronic Component and Technology Conference, pp. 884-890, March 30-June 2, San Diego, CA.

[53] Deng, X., G. Piotrowski, J. Williams, and N. Chawla, "Influence of Initial Morphology and Thickness of Cu6Sn5 Intermetallics on Growth and Evolution During Thermal Aging of Sn-Ag Solder/Cu joints," Journal of Electronic Materials, Vol. 32, No. 12, pp. 1403-1413, 2003.

[54] Pang, J., X. Luhua, X. Shi, W. Zhou. and S. Ngoh., "Intermetallic Growth Studies on Sn-Ag-Cu Lead-free Solder Joints," Journals of Electronic Materials, Vol. 33, No. 10, pp. 1219-1226, 2004.

[55] Valota A.T., Losavio A., Renard L. and Vicenzo A., "High Speed Pull Test Characterization of BGA Solder Joints", 7th International Conference on Thermal, Mechanical and Multiphysics Simulation and Experiments in micro-electronics and Micro-Systems, EuroSime 2006, pp. 1-6, 24th – 26th April, 2006.

[56] Yang W., Messler R.W. and Felton L.E., "Microstructure evolution of Eutectic Sn-Ag Solder Joints", Journal of Electronic Materials, Vol. 23, No. 8, pp. 765-772, 1994.

[57] Allen S.L., Notis M.R., Chromik R.R., Vinci R.P., Lewis D.J., and Schaefer R., “Microstructural Evolution in Lead-free Solder Alloys: Part II-Directionally Solidified Sn-Ag-Cu, Sn-Cu, Sn-Ag, Journal of Materials Research, Vol. 19, No. 5, pp. 1425-1431, May 2004.

[58] Zhang, Q., A. Dasgupta. and P. Haswell, “Isothermal Mechanical Creep and Fatigue in Pb-free Solders,” Proceedings of International Brazing & Soldering Conference, San Diego, CA, February 16-19, 2003

[59] Henderson, D. J, et al., “The Microstructure of Sn in Near Eutectic Sn-Ag-Cu Alloy Solder Joints and Its Role in Thermomechanical Fatigue,” Journal of Materials Research, Vol. 19, No. 6, pp. 1608-1612, June 2004.

[60] Lee, T. Y., Choi W. J., Tu K. N., Jang J. W., Kuo S. M., Lin J. K., Frear D. R., Zeng K. and Kivilahti J. K., "Morphology, Kinetics, and Thermodynamics of Solid-State Aging of Eutectic SnPb and Pb-Free Solders (Sn-3.5Ag, Sn-3.8Ag-0.7Cu And Sn-0.7Cu) on Cu," Journal of Materials Research, Vol. 17, pp. 291-301, 2002.

[61] Wu, Ji and Ganesan, S., “Using Cut-out Features for Efficient Printed Circuit Board Testing and Failure Analysis,” IEEE Transactions on Component and Packaging Technology, vol. 28, issue 1, March 2005, pp. 166-168.

[62] Japanese Industry Standard JIS Z 3198 - 6, “Test Method for Lead-free Solders – Part 6: Methods for 45º Pull Test of Solder Joints on QFP Lead,” Tokyo, Japan, Dec 2003.

[63] NIST, “Database for Solder Properties with Emphasis on New Lead-free Solders”, http://www.boulder.nist.gov/div853/lead%20free/solders.html, 06/2006

[64] Chang K.C. and Chiang K.N., “Aging Study on Interfacial Microstructure and Solder-Ball Shear Strength of a Wafer-Level Chip-Size Package with Au/Ni Metallization on a Cu Pad”, Journal of Electronic Materials, pp. 1373-1380, Vol. 33, No. 11, 2004

[65] T. T. Mattila, V. Vuorinen, and J. K. Kivilahti, "Impact of printed wiring board coatings on the reliability of lead-free chip-scale package interconnections", Journal of Materials Research, , pp. 3214-3223., Vol. 19, No. 11, 2004